eLife

Reviewed Preprint
v1 • March 3, 2026
Not revised

Reviewed Preprint
v2 • May 29, 2026
Revised by authors

For correspondence:
j.k.eykelenboom@dundee.ac.uk
t.tanaka@dundee.ac.uk

†, ‡, * Author notes: See page 26

Funding: See page 26

Reviewing editor: Silke Hauf, Virginia Tech, United States

© 2026, Sheidaei et al. This article is distributed under the terms of the Creative Commons Attribution License, which permits unrestricted use and redistribution provided that the original author and source are credited.

Contractile perinuclear actomyosin network promotes peripheral and polar chromosome interaction with the mitotic spindle

Nooshin Sheidaei[*,†], **John K Eykelenboom**[*], **Zuojun Yue**, **Graeme Ball**, **Alexander JR Booth**[‡], **Tomoyuki U Tanaka**

Division of Molecular, Cell and Developmental Biology, School of Life Sciences, University of Dundee, Dundee, United Kingdom

eLife Assessment

This **important** study demonstrates that a perinuclear actomyosin network, present in some types of human cells, facilitates kinetochore-spindle attachment of chromosomes in unfavorable locations, thereby reducing their missegregation rate. This actomyosin network and its general role have been studied previously, but this study **convincingly** clarifies the underlying mechanism and expands the investigation to additional cell lines. The results are relevant to understanding chromosome missegregation in cancer cells.

[Editors' note: this paper was reviewed by *Review Commons*.]

https://doi.org/10.7554/eLife.110952.2.sa3

Abstract

Chromosomes must efficiently and properly interact with the mitotic spindle during prometaphase for correct segregation. Chromosomes at the nuclear periphery or behind the spindle poles interact less efficiently with the mitotic spindle, increasing the risk of missegregation during anaphase. The mechanisms that mitigate such risks in unperturbed cells are unknown. An actomyosin network (PANEM) forms around the nucleus during prophase. While the myosin-II-dependent PANEM contraction facilitates chromosome interaction with the mitotic spindle following nuclear envelope breakdown (NEBD), the mechanism by which it does so remains unclear. Here, using human cell lines, we show that immediately after NEBD, PANEM contraction directly pushes chromosomes at the nuclear periphery toward the centre. Detailed tracking of kinetochore movements following light-induced activation of a myosin-II inhibitor reveals that this inward movement facilitates kinetochores' initial interaction with spindle microtubules. PANEM contraction also promotes the onset of their congression towards the spindle mid-plane, but not congressional motion itself. Furthermore, PANEM contraction reduces the volume of polar regions, helping reposition chromosomes and initiate their congression. Thus, PANEM contraction ensures high-fidelity chromosome segregation by relocating chromosomes from unfavorable locations. Some chromosomally unstable cancer cells fail to establish PANEM during early mitosis, implying its absence in cancer progression.

Introduction

For high-fidelity chromosome segregation in human cells, all chromosomes must correctly interact with microtubules (MTs) of the mitotic spindle during the early stage of mitosis (prometaphase), i.e. shortly after nuclear envelope breakdown (NEBD). To facilitate this, the bipolar mitotic spindle is established when two spindle poles separate from each other around the time of NEBD [1], while the kinetochore provides the major MT interaction site on a chromosome [2,3,4]. The kinetochore

interacts with MTs emanating from spindle poles in a stepwise manner [5,6]: it initially interacts with the lateral side of a MT and then travels along it towards a spindle pole, before it attaches to the plus end of the same MT after this MT shrinks [7–10,11]. The other sister kinetochore then interacts with the side of another MT (either another kinetochore-attached MT or a pole-to-pole MT) and moves along it towards the middle of the mitotic spindle (spindle mid-plane or metaphase plate) in a process called chromosome congression [12,13]. Finally, biorientation is established when one of the sister kinetochores interacts with MTs only from one spindle pole and the other sister kinetochore with MTs only from the opposite pole. [6,14], leading to the oscillatory motions of chromosomes around the spindle mid-plane [15–17].

For efficient and correct kinetochore-MT interaction, the locations of chromosomes in the nucleus (when NEBD occurs) or relative to spindle poles (after NEBD occurs) are crucial. For example, chromosomes at the nuclear periphery or behind spindle poles (polar regions) early in mitosis show higher risk of missegregation during the subsequent anaphase than other chromosomes [18,19]. In other words, these chromosomes' locations in early mitosis are unfavorable for correct segregation later in mitosis. It is thought that (1) chromosomes at the nuclear periphery are located further away from spindle poles and therefore require a longer time to interact with spindle MTs extending from spindle poles, and (2) chromosomes at polar regions require a longer time to start congression to the spindle mid-plane [18,19]. Nevertheless, the missegregation rate of these chromosomes is still relatively low in unperturbed normal cells, meaning there might be mechanisms mitigating the risks of missegregation for chromosomes found at these locations. However, such mechanisms have not yet been identified.

Recently, potentially relevant to such mechanisms, a LINC complex-dependent actomyosin network that is rapidly formed on the cytoplasmic side of the nuclear envelope (NE) during prophase was reported [20,21] (Figure 1A). In the current study, we call this actomyosin network PANEM (**P**erinuclear **A**ctomyosin **N**etwork in **E**arly **M**itosis). The PANEM is formed in U2OS and RPE1 cells, but not in HeLa cells [20,21]. In prophase, the PANEM facilitates the separation of spindle poles to establish a bipolar spindle [21]. Following NEBD, the PANEM remains on the NE remnants for 10-15 min and shows contraction promoted by myosin II [20] (Figure 1A). Concomitantly, chromosome scattering volume (CSV), quantified by three dimensional convex hull fitting [20], also becomes smaller (Figure 1B). The reduction in CSV after NEBD also occurred after MT disruption with nocodazole treatment, suggesting that it was not dependent on chromosome interaction with spindle MTs [20]. It was concluded that the myosin II-dependent PANEM contraction promoted CSV reduction. Furthermore, in situations where PANEM contraction was inhibited, (1) chromosomes often remained in polar regions, (2) anaphase onset was frequently delayed, and (3) chromosome missegregation often occurred [20] (Figure 1 – figure supplement 1). The PANEM contraction seemed to facilitate correct chromosome interaction with spindle MTs. However, it has been unclear how PANEM contraction promotes the stepwise development of kinetochore interaction with spindle MTs mentioned above or which chromosomes specifically benefit from the PANEM contraction in this process.

In this work, we address which steps of kinetochore-MT interaction are facilitated by the PANEM contraction and which kinetochores are helped by the PANEM contraction to establish correct MT interaction. We find that soon after NEBD, the PANEM contraction assists kinetochores at the nuclear periphery in initiating interaction with spindle MTs.

Moreover, the PANEM contraction helps the kinetochores in polar regions (i.e. behind spindle poles) to start congression towards the middle of the mitotic spindle. The PANEM contraction has such effects because it pushes chromosomes inward, thus repositioning them to facilitate their correct interaction with spindle MTs. Therefore, PANEM contraction repositions chromosomes from unfavorable locations to establish their correct interaction with spindle MTs, thus mitigating the risks of their missegregation later in mitosis. In this study, we also broaden our analysis of PANEM to multiple human cell lines. While PANEM was also found to be required for reducing CSV in a human non-cancerous cell line, several cancer cells with high levels of aneuploidy were found to lack PANEM in early mitosis. This suggests a link between PANEM and numerical chromosomal instability (N-CIN), which is associated with cancer progression.

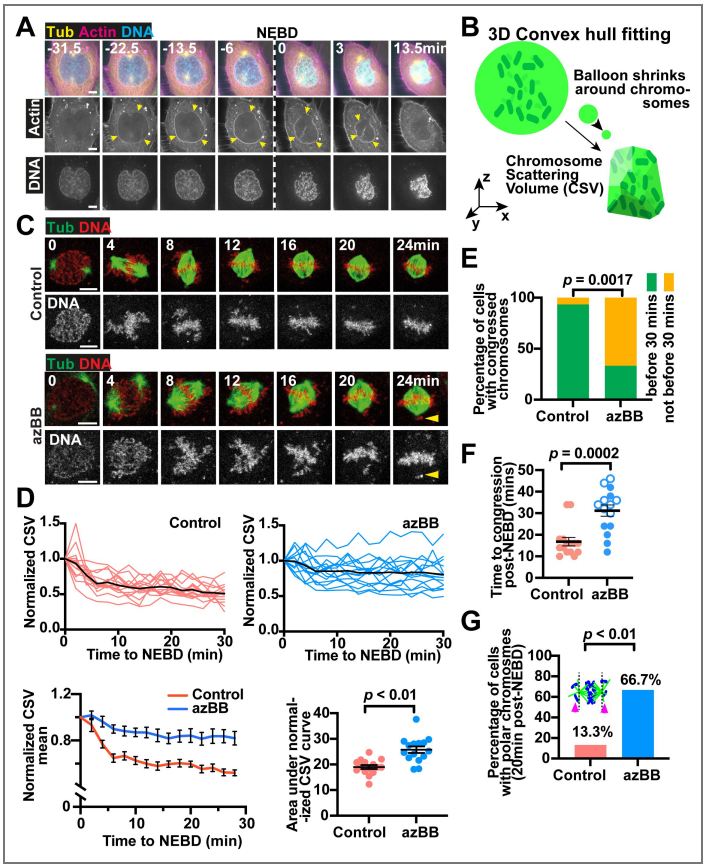

Figure 1. The outcome of selective and rapid suppression of perinuclear actomyosin network (PANEM) contraction.

(A) Time-lapse images show a representative cell passing through the early stages of mitosis (prophase and prometaphase). A stable cell line expressing mCherry-LifeAct and GFP-αTubulin, with chromosomes visualized by SYTO deep-red was imaged every 1.5 minutes. The timing of nuclear envelope breakdown (NEBD) is indicated by the dotted line. The PANEM is indicated by yellow arrowheads. Scale bar is 5μm. **(B)** Diagram shows how the chromosome scattering volume (CSV) was defined. The convex-hull was fitted in three dimensions (3D) to represent chromosome distribution. A hypothetical 'balloon' (green) shrinks around chromosomes (dark green) in 3D to create a convex hull or a minimal polyhedron wrapping chromosomes. The volume of the 3D convex hull indicates how widely chromosomes are scattered in space. **(C)** Time-lapse images show representative cells passing through mitosis (prometaphase to metaphase). A stable cell line expressing GFP-αTubulin, with chromosomes visualized by SiRDNA, was imaged every 4 minutes following treatment with or without azBB followed by nuclear irradiation using a 2-photon 860nm laser. NEBD occurred at 0 minute and was detected by diffusion of free GFP-αTubulin into the nuclear space. Chromosomes that did not congress and lie behind the spindle poles are indicated by yellow arrowheads. Scale bar is 10μm. Time-lapse images, exemplified here, were used in the analyses in D–G. **(D)** Graphs in the upper panels show normalized chromosome scattering volume (CSV; see B) before and after NEBD (0 min) for cells treated with or without azBB. The data is normalized to the volume at 0 minutes (immediately after NEBD). Each red or blue line represents the measurements from an individual cell while the heavy black lines represent the mean measurement across the time points. In the lower left panel the mean of normalized values obtained above are presented here again with standard error of mean (SEM) shown for each time point for each condition. In the lower right panel, the graph plot the areas under the curves for normalized CSV, measured in individual cells. The bars represent the mean and SEM. The *p* value was obtained using t-test. The data without normalization is shown in Figure 1 – figure supplement 3. **(E)** Graph shows the percentage of cells, treated either with or without azBB, whose chromosomes were congressed before 30min (green) or not (orange). The number of cells for each group was 15. The *p* value was obtained using Fisher's exact test. **(F)** Graph shows the time (from NEBD) taken for completion of congression in individual cells treated either with or without azBB. Open circle data points represent cells that had not completed congression at the end of the time lapse sequence. The bars represent the mean and SEM. The *p* value obtained using an unpaired Mann-Whitney test. **(G)** Graph shows the percentage of cells which exhibited chromosomes behind the spindle poles 20 minutes after NEBD. The cartoon shows microtubules (green), boundaries for polar regions (the black dotted lines), chromosomes (blue), and polar chromosomes (pink arrowheads). The number of cells analyzed for each group was 15. The *p* value was obtained using Fisher's exact test.

Results

Developing a method for selective and prompt suppression of the PANEM contraction soon after NEBD

We aimed to study how PANEM contraction facilitates chromosome interaction with spindle MTs, including their initial interaction. Our previous data and other studies suggested the initial chromosome interaction with spindle MTs occurs within 8 min of NEBD [5,20,22–25].

Therefore, we aimed to suppress PANEM contraction within this time range and study the outcome. While the PANEM contour becomes ambiguous about 10 min after NEBD, the CSV reduction reflects the extent of PANEM contraction for a longer time [20] (see Introduction). To suppress the PANEM contraction and CSV reduction, we previously used para-nitro-blebbistatin (pnBB), an inhibitor of myosin-II [20]. However, this suppression was only apparent after 8 min following NEBD. We suspected the delayed effect was due to the partial inhibition of the myosin II activity by pnBB.

In the current study, to suppress the myosin II activity more efficiently, we used azido-blebbistatin (azBB). When excited with two-photon infrared light, azBB covalently binds the heavy chain of myosin II and inhibits its ATPase activity [26,27]. We used a low concentration of azBB to ensure that myosin II was inhibited only at the region exposed to infrared light in U2OS cells. To inhibit myosin II on the PANEM, only the nucleus was irradiated by the infrared light during prophase, avoiding the cell cortex where a high amount of myosin II localizes [28]. In the control, the nucleus was also irradiated by infrared light, but without azBB treatment. We confirmed that cell rounding during mitosis, which requires myosin II at the cell cortex [28], occurred similarly between the azBB treatment and the control (Figure 1 – figure supplement 2). This suggests that, as intended, myosin II of the cell cortex remained functional.

To enrich prophase cells, we arrested U2OS *cdk1-as* cells (with GFP-αTubulin) at the end of G2 phase by treating them with an ATP analogue 1NM-PP1 [20,21]. After 1NM-PP1 washout, these cells entered mitosis synchronously, and chromosomes were visualized with SiRDNA. The nuclei of prophase cells (those showing partial chromosome condensation) were exposed to infrared light in the presence and absence of azBB (Figure 1C), and the change of CSV was measured over time (Figure 1D, Figure 1 – figure supplement 3). NEBD was identified by the influx of GFP-αTubulin signals (not incorporated into MTs) from the cytoplasm into the nucleus. In the control cells (without azBB), CSV reduction occurred rapidly until 6 min after NEBD and more slowly for the next 10 min or so (Figure 1D) – these results are consistent with the previous report [20]. With azBB, the CSV reduction was weakened, compared with control cells – the difference was significant from 4 min after NEBD and onwards (Figure 1D). Treatment of cells with nocodazole (with and without azBB) before irradiation did not affect the outcomes, suggesting that the effect of azBB was independent of MTs (Figure 1 – figure supplement 4). Moreover, we also measured the volume inside the PANEM with and without azBB – the reduction of this volume was also weakened with azBB treatment within 8 min after NEBD (Figure 1 – figure supplement 5).

Furthermore, we previously showed that the suppression of the PANEM contraction with pnBB led to (1) a delay in chromosome congression and anaphase onset, (2) an increase of chromosomes at the polar region (behind spindle poles), leading to chromosome missegregation [20]. These defects were also observed after the PANEM contraction was suppressed with azBB treatment (Figure 1E-G). Although these problems might have resulted from spindle assembly defects, a comparison of spindle length between the two conditions suggests this was not the case (Figure 1 – figure supplement 6), indicating that the spindle assembly was largely normal after the PANEM contraction was suppressed with azBB.

In summary, both the PANEM contraction and consequent CSV reduction were dependent on the activity of myosin II, and both occurred shortly (within 8 min) after NEBD. Both events can be suppressed by treatment with the myosin II inhibitor azBB within this time range.

Therefore, we decided to use azBB to rapidly suppress the PANEM contraction following NEBD and study how this affects chromosome interactions with spindle MTs (see below).

Kinetochore-MT interaction is developed through four distinct phases during prometaphase

The kinetochore provides the main MT attachment site on a chromosome. To investigate the effect of PANEM contraction on kinetochore-MT interaction, we first sought to distinguish the sequential phases through which this interaction is developed and established. For this, U2OS cells were synchronized as in the previous section, and we imaged the kinetochore (CENP-B-mCherry) and MTs (GFP-αTubulin) every 30 s. We were able to track the positions of individual kinetochores over time if they were not too crowded (Figure 2 – figure supplement 1). We then tracked the position of each of these kinetochores, over time, relative to the following three reference points: (1) the midpoint between spindle poles, (2) the mid-plane between spindle poles, and (3) a spindle pole (the one towards which the kinetochore moved after NEBD) (Figure 2A).

We first analyzed how the positions of kinetochores changed over time in control cells (i.e. without azBB), following NEBD. Although such changes varied among individual kinetochores, we identified the following two common features for individual kinetochores (Figure 2B, C): First, after a few minutes following NEBD, kinetochores moved rapidly towards one of the two spindle poles, i.e. the distance to a spindle pole was rapidly shortened (Figure 2B, C; pale blue area). This poleward kinetochore motion started immediately after the initial kinetochore interaction with a MT extending from the spindle pole. The poleward kinetochore motion likely reflects the rapid kinetochore motion along the lateral side of a MT, as previously reported [7,9].

Second, after a few minutes following the completion of the poleward kinetochore motion, the kinetochore moved towards the mid-plane between spindle poles, i.e. the distance to the spindle pole was enlarged while the distance to the spindle mid-plane was shortened (Figure 2B, C; pale yellow area). This kinetochore motion seemed to reflect chromosome congression to the spindle mid-plane [12,13]. Such kinetochore motion continued for a few minutes and, once the kinetochore came close to the spindle mid-plane, it started oscillatory motions around the metaphase plate.

Based on the above motions of individual kinetochores, we defined Phase 1–4 as follows (Figure 2C): Phase 1 was the period between NEBD and the start of the poleward kinetochore motion – the latter also matched the initial kinetochore-MT interaction (based on co-localization of CENP-B and MT signals). Phase 2 was the kinetochore motion towards a spindle pole (see above). Phase 3 was defined as the period between Phase 2 and the start of kinetochore motion towards the spindle mid-plane. Phase 3 was often short in control cells and, during Phase 3, no common characteristic kinetochore motions (e.g. directional motions) were observed. Phase 4 was defined as the kinetochore motion towards the spindle mid-plane (see above).

We then analyzed the change of kinetochore positions over time in azBB-treated cells (Figure 2D). After a few minutes following NEBD, rapid kinetochore motions towards a spindle pole were observed, which was defined as Phase 2, as in control cells. This allowed us to define Phase 1 (the period between NEBD and the start of Phase 2) and Phase 3 (its start was the end of Phase 2) in the same way for azBB-treated and control cells. However, for some kinetochores in azBB-treated cells, the kinetochore motion towards the spindle mid-plane (defined as Phase 4) occurred after a long delay (Figure 2D, top) or did not occur during observation (Figure 2D, bottom). Next, using this data, we conducted a detailed comparison of kinetochore motions during each phase between control and azBB-treated cells.

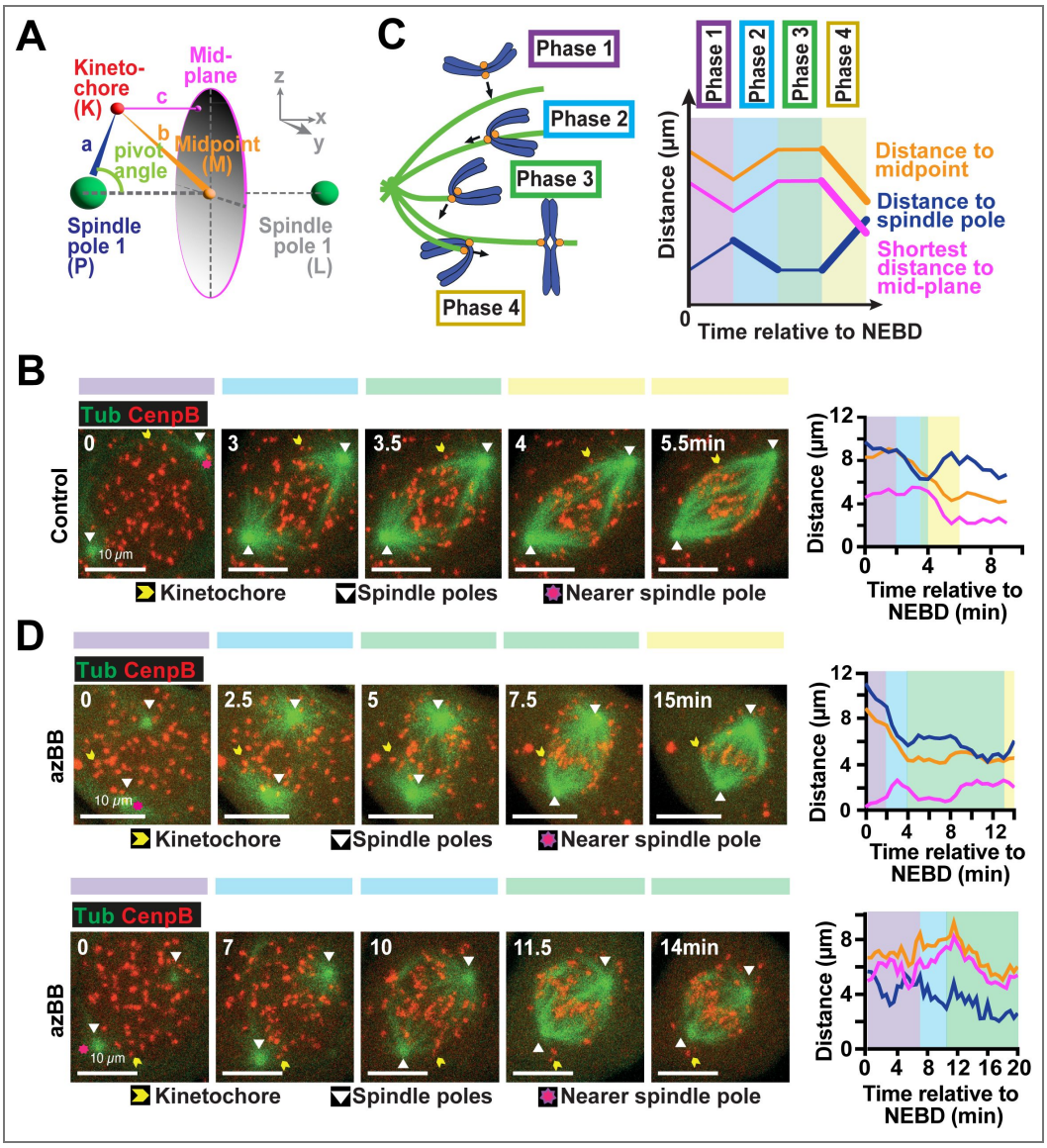

Figure 2. Tracking kinetochores during early phases of mitosis reveals four major phases of motion leading to congression to the spindle mid-plane.

(A) To assess kinetochore motions during early mitosis (prometaphase), distances were calculated between the kinetochore and the nearest spindle pole, the spindle mid-point and the metaphase plate (mid-plane). To assess the location of the kinetochore relative to the spindle poles (polar or non-polar), the pivot angle was calculated. Designated color codes for each distance are indicated in the diagram. **(B)** Time-lapse images show a representative control cell passing through the early stages of mitosis (prometaphase). A stable cell line expressing CENPB-mCherry and GFP-αTubulin was imaged every 30 seconds. The spindle poles are indicated by white arrowheads. The tracked kinetochore is indicated in each frame by a yellow arrowhead. The nearest spindle pole is indicated by a magenta star in the first image of the sequence. Scale bar is 10µm. The graph on the right-hand side indicates the distance of the indicated kinetochore to the nearest spindle pole (dark blue line), the spindle midpoint (orange line) and the spindle mid-plane (magenta line). The colored boxes on the graph, and above the images on the left-hand side, represent the different phases of motion (explained in C). **(C)** Kinetochore tracking revealed four distinct phases of motion as summarized in the cartoon on the left-hand side (described in detail in the main text). The bold lines in the theoretical graph on the right-hand side show the characteristic changes in distance to the different cellular locations (indicated in A) for the four phases. Phase 2 is characterized by rapid reduction in distance to the nearest spindle pole while Phase 4 by increase in distance to the spindle pole and reduction in distance to the midpoint and mid-plane. Color coding for each phase is indicated by the colored frames and boxes in the cartoon and the graph. **(D)** Time-lapse images show two representative cells passing through the early stages of mitosis (prometaphase). Cells were as described in B except they were treated with azBB. The features of the graphs on the right-hand side of the time-lapse sequences are as described in B.

The PANEM contraction facilitates the initial interaction of peripheral kinetochores with spindle MTs, but not their subsequent poleward motions

While the PANEM showed contraction after NEBD, it seemed that peripheral kinetochores, i.e. those localizing near the nucleus-cytoplasm boundary at NEBD, moved inward (see below). We hypothesized that the effect of PANEM contraction on kinetochore-MT interaction is greater for peripheral kinetochores than for the kinetochores localizing to the central part of the nucleus at NEBD (central kinetochores). Therefore, to study kinetochore-MT interaction, we analysed peripheral and central kinetochores separately: the former was defined as kinetochores localizing within 2 μm of the nucleus-cytoplasm boundary at NEBD while the latter were the other kinetochores (Figure 3A). Kinetochore motions in Phase 1-4 were defined as in the previous section and in the same way for peripheral kinetochores (Figure 2B, D; Figure 2 – figure supplement 1A) and central kinetochores (Figure 2 – figure supplement 1B, C).

Figure 3B shows examples of how the positions of peripheral kinetochores (after NEBD) changed over time, relative to the spindle pole (towards which the kinetochore moved during Phase 2), in control and azBB-treated cells. We first analyzed Phase 1 of the kinetochore motion. To investigate the effect of PANEM contraction on the initial kinetochore interaction with spindle MTs, we measured the duration of Phase 1. For peripheral kinetochores, Phase 1 was significantly longer in azBB-treated cells than in control cells (Figure 3C, left). By contrast, for central kinetochores, the duration of Phase 1 was not significantly different between azBB-treated cells and control cells (Figure 3C, right). This suggests that the PANEM contraction promotes the initial interactions of peripheral kinetochores, but not central kinetochores, with spindle MTs.

If PANEM contraction pushes peripheral chromosomes inward during Phase 1, the associated peripheral kinetochores may travel inward for a larger distance than central kinetochores. However, no significant difference was observed between azBB-treated and control cells, in the travel distance of peripheral kinetochores towards the mid-point of spindle poles during Phase 1 (Figure 3D, top, left). Central kinetochores also did not show a significant difference (Figure 3D, bottom, left). However, the travel distance measurement might be biased since the period of Phase 1 for peripheral kinetochores was shorter in control cells than in azBB-treated cells (Figure 3C, left). Since, on average, Phase 1 finished earlier in control cells, peripheral kinetochores had overall less time to travel. To avoid this potential bias in our comparison, we measured the travel distance of kinetochores before they interacted with spindle MTs, during the fixed time windows of 2, 2.5, 3 or 4 min following NEBD, i.e. once they interacted with spindle MTs within each time window, they were not included in the analyses. For peripheral kinetochores, their inward travel distance was significantly longer in control cells than in azBB-treated cells across the fixed time windows 2.5, 3 and 4 min (Figure 3D, top, right). By contrast, central kinetochores did not show such a difference (Figure 3D, bottom, right). These results suggest that the PANEM contraction moves peripheral kinetochores inward, but not central kinetochores, during Phase 1. We reason that such inward motions of peripheral kinetochores facilitate their initial interaction with spindle MTs, i.e. shorten the duration of Phase 1.

We next analyzed the kinetochore motions in control and azBB-treated cells during Phase 2. We found that the duration of Phase 2 was shorter for central kinetochores than for peripheral kinetochores (Figure 3E). However, there was no significant difference in the duration of Phase 2 between control and azBB-treated cells, for either the peripheral or central kinetochores (Figure 3E). We also analyzed the kinetochore travel distance towards the closest spindle pole during Phase 2, i.e. the difference in the distance to the spindle pole at the start and end of Phase 2. The kinetochore travel distance was shorter for central kinetochores than for peripheral kinetochores (Figure 3F). However, it showed no significant difference between control and azBB-treated cells, for peripheral or central kinetochores (Figure 3F). In addition, there was no significant difference in the average speed of the poleward motions between control and azBB-treated cells,

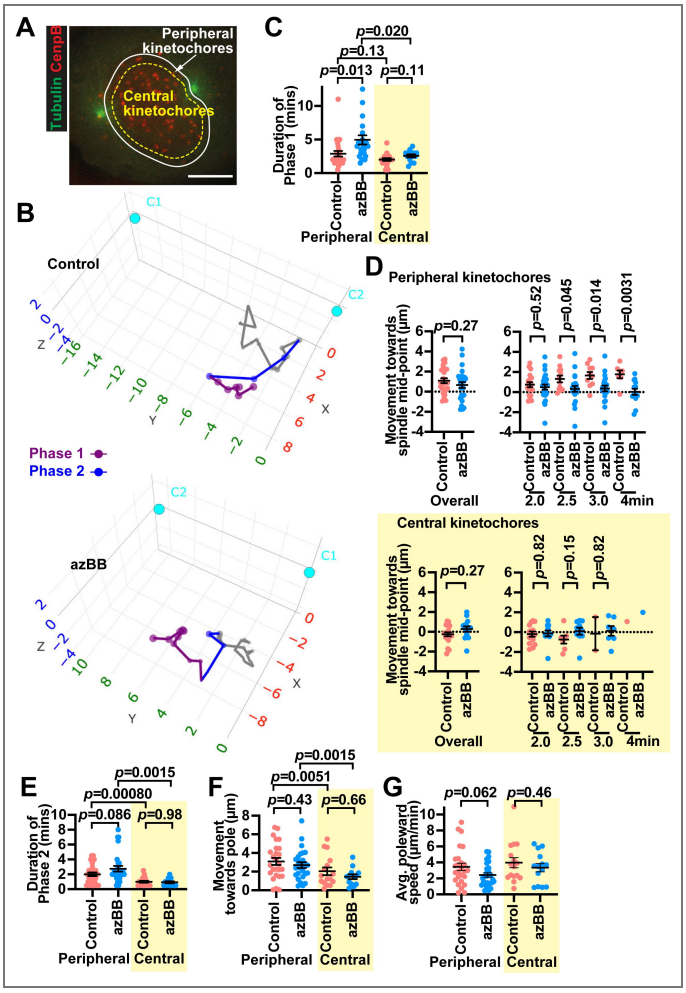

Figure 3. Reduced PANEM contraction affects motions of peripheral (but not central) kinetochores during Phase 1.

(A) Image shows a cell in late prophase expressing CENPB-mCherry and GFP-αTubulin. The white line indicates the position of the nuclear membrane. Kinetochores that fell within the yellow dotted line (positioned 2µm inside the nucleus) were considered central kinetochores, those between the two lines were considered peripheral kinetochores. There were a small number of non-kinetochore-derived mCherry signals, which localized outside the nucleus before NEBD and did not show any characteristic kinetochore motions, such as those towards a spindle pole and the spindle mid-plane, after NEBD. Scale bar is 10µm. **(B)** The motions of representative kinetochores are shown in 3D space over time in control cells (top) or azBB-treated cells (bottom). Kinetochores (colored dots) and spindle poles (turquoise circles) were tracked as in Figure 2 and positions were plotted relative to the nearest spindle pole (C2 in upper panel, C1 in lower panel) which was positioned at x=0, y=0, z=0. The position of the opposite spindle pole represents the average relative position of the pole during the time sequence. The colored lines of the kinetochore track represent Phase 1 (purple), Phase 2 (blue) as in Figure 2C. Phases 3 and 4 are shown in grey. The scales on all three axes are in µm. **(C)** Graph shows the duration of Phase 1 for individual kinetochores from control (red) or from azBB-treated (blue) cells. Kinetochores from the periphery are shown on the left-hand side and those from the centre on the right-hand side with a yellow-colored box. The *p* values were obtained by t-test. 26, 27, 20 and 14 kinetochores (from 9, 9, 6 and 7 cells) were analyzed from left to right. Note that in the peripheral azBB-treated column one kinetochore took 17.5 minutes before entering phase 2 and is excluded from this graph. **(D)** Graph shows the distance moved towards the spindle mid-point during Phase 1 for individual kinetochores from control (red) or from azBB-treated (blue) cells. In each panel, the graph on the left-hand side shows the net change in distance of individual kinetochores towards the spindle mid-point, while the graphs on the right-hand side show the net change in distance during the indicated time period (relative to NEBD) for the subset of kinetochores that had not interacted with MTs during that period. The *p* values were obtained by t-test. **(E-G)** Graphs show the duration of Phase 2 (E), movement towards the nearest pole during Phase 2 (F) and the average poleward speed during Phase 2 (G) for individual kinetochores from control (red) or from azBB-treated (blue) cells. The source data for these analyses (coordinates of kinetochores and spindle poles) can be found in Figure 3 – source data 1 - 4.

for peripheral or central kinetochores (Figure 3G). These results suggest that, while the PANEM contraction advances the onset of Phase 2, it does not affect the processes that occur during Phase 2.

The PANEM contraction helps peripheral kinetochores to start congression towards the spindle mid-plane, but does not promote their congressional motion itself

Figure 4A shows examples of how peripheral kinetochores subsequently changed their positions over time after NEBD, with Phase 3 and 4 motions highlighted. We analyzed Phase 3 of the kinetochore motions in control and azBB-treated cells. As expected, the start of Phase 3, relative to NEBD, was significantly delayed in azBB-treated cells (compared with control cells) for peripheral kinetochores, due to their extended Phase 1 (Figure 4B).

We next assessed the duration of Phase 3 in control and azBB-treated cells. In both conditions, the duration of Phase 3 was less than 5 min for all central kinetochores (Figure 4C). It was also less than 5 min for most peripheral kinetochores in control cells. However, for most peripheral kinetochores after azBB treatment, Phase 3 duration was longer than 5 min (Figure 4C). In many of them, we did not observe the end of Phase 3, i.e. the kinetochore motion towards the spindle mid-plane (Phase 4) did not start (Figure 4C, open circles). On the other hand, during Phase 3, there was no significant change in the kinetochore positions (relative to a spindle pole) in control or azBB-treated cells for peripheral or central kinetochores (Figure 4D), as we may expect from the definition of Phase 3 (i.e. the interval between Phase 2 and Phase 4). In summary, when the PANEM contraction was inhibited, Phase 3 was significantly extended for many peripheral kinetochores, but not for central kinetochores.

We then analysed the kinetochore motions during Phase 4, i.e. congression towards the spindle mid-plane (Figure 4A). The start of Phase 4 (relative to NEBD) was similar in control and azBB-treated cells for central kinetochores (Figure 4E), but it was significantly delayed for many peripheral kinetochores in azBB-treated cells (compared with control cells) (Figure 4E), which is explained by their extended Phase 1 and Phase 3. In contrast, once Phase 4 started, there was no significant difference in the duration of Phase 4 for peripheral or central kinetochores between control and azBB-treated cells (Figure 4F). There was also no significant difference in the kinetochore travel distance or the average congression speed during Phase 4 between control and azBB-treated cells (Figure 4G, H). In short, in this analysis, a clear effect of inhibition of PANEM contraction was the failure (or delay) of several peripheral kinetochores to begin congression. However, if and once congression began, peripheral kinetochores (and central kinetochores) showed no significant change in motions of congression after the PANEM contraction was inhibited.

Summarizing the analyses of Phases 1-4 in the previous and current sections, the durations of Phase 1 and Phase 3 were extended for peripheral kinetochores, but not for central kinetochores, when PANEM contraction was inhibited with azBB (Figure 4I). The inward travel distance was shortened for peripheral kinetochores (but not for central kinetochores) during Phase 1 after azBB treatment (Figure 4I). In addition, the starts of Phases 2, 3 and 4 were delayed for peripheral kinetochores, which we interpret as the secondary effects of extended Phases 1 and 3.

So far, we randomly selected peripheral and central kinetochores in both polar and non-polar regions at NEBD (Figure 3A and 5A). Since polar regions were generally smaller than non-polar regions, most of our selected peripheral kinetochores were in non-polar regions (while all selected central kinetochores were in non-polar regions). Next, we repeated our analyses of Phases 1-4 only for the peripheral kinetochores specifically in non-polar regions (Figure 4 – figure supplement 1). The results for non-polar kinetochores were still essentially the same as in Figures 3 and 4.

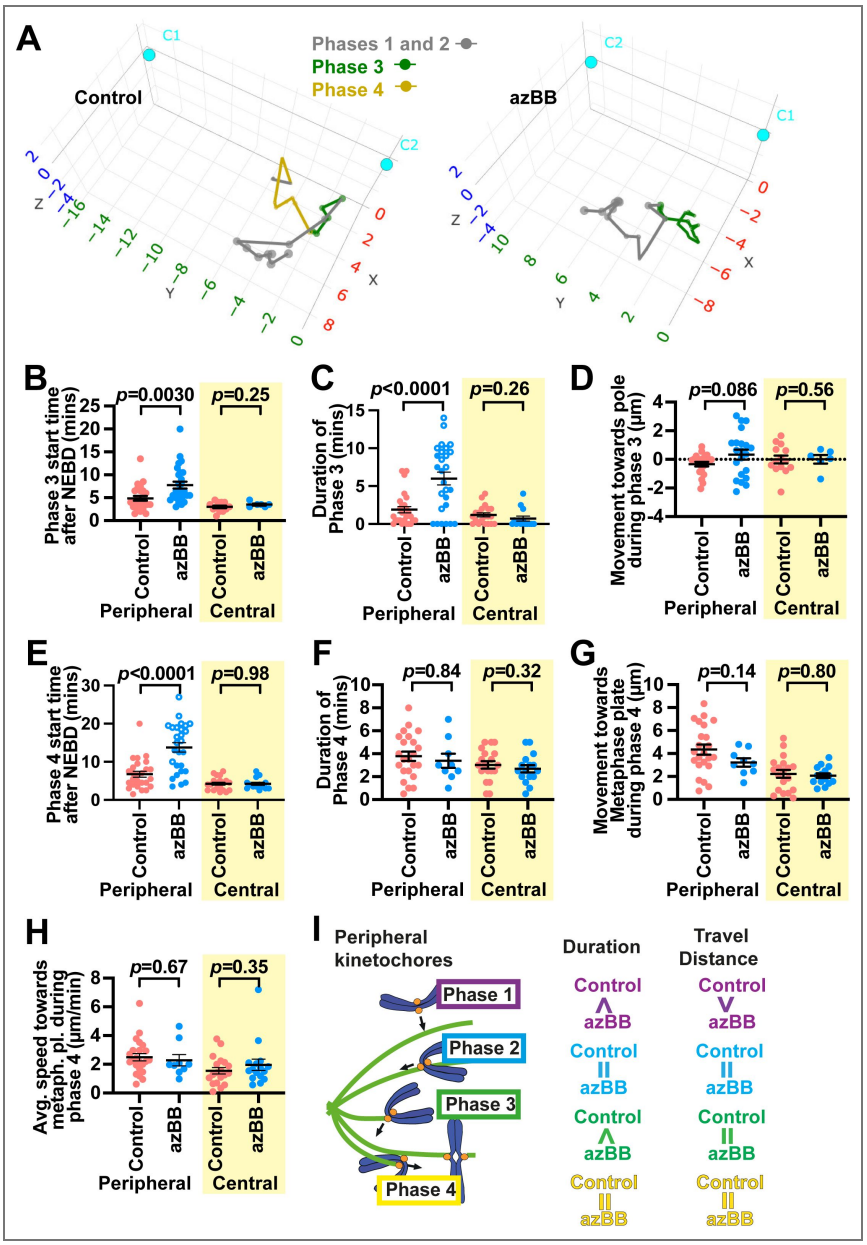

Figure 4. Reduced PANEM contraction leads to a delay in, or absence of, congressional movement of peripheral kinetochores.

(A) The motions of representative kinetochores are shown in 3D space over time in control cells (left) or azBB-treated cells (right), as in Figure 3B. The colors of the kinetochore track represent Phase 3 (green), Phase 4 (yellow) as described in Figure 2C. The scales on all three axes are in µm. The same kinetochores as in Figure 3B are shown here. **(B–E)** Graphs shows the start time of Phase 3 relative to NEBD (B), duration of Phase 3 (C), net change in distance relative to the nearest spindle pole (difference between the start and end of Phase 3 [or the end of observation if congression did not start during observation]; D), and the start of Phase 4 relative to NEBD (or the end of observation if congression did not start during observation; E) for individual kinetochores from control (red) or from azBB-treated (blue) cells. The *p* values were obtained by t-test. 26, 27, 20 and 14 kinetochores (from 9, 9, 6 and 7 cells) were analyzed from left to right. Open circles indicate kinetochores that did not start congression (the end of Phase 3 was not defined). **(F–H)** Graphs show the duration of Phase 4 (F), net change in distance relative to the spindle mid-plane during Phase 4 (G) and the average speed during Phase 4 (H) for individual kinetochores from control (red) or from azBB-treated (blue) cells. The *p* values were obtained by t-test. 23, 9, 19 and 14 kinetochores (from cells corresponding to B-E) were analyzed from left to right. **(I)** Summary of comparison between control and azBB-treated cells for peripheral kinetochore motions during early mitosis (prometaphase). Similarities (equal sign) or differences (greater than or less than sign) are shown between control and azBB-treated cells. When a phase starts later, it is indicated by a 'greater' sign. Red asterisks indicate presumed direct effects of reduced PANEM contraction.

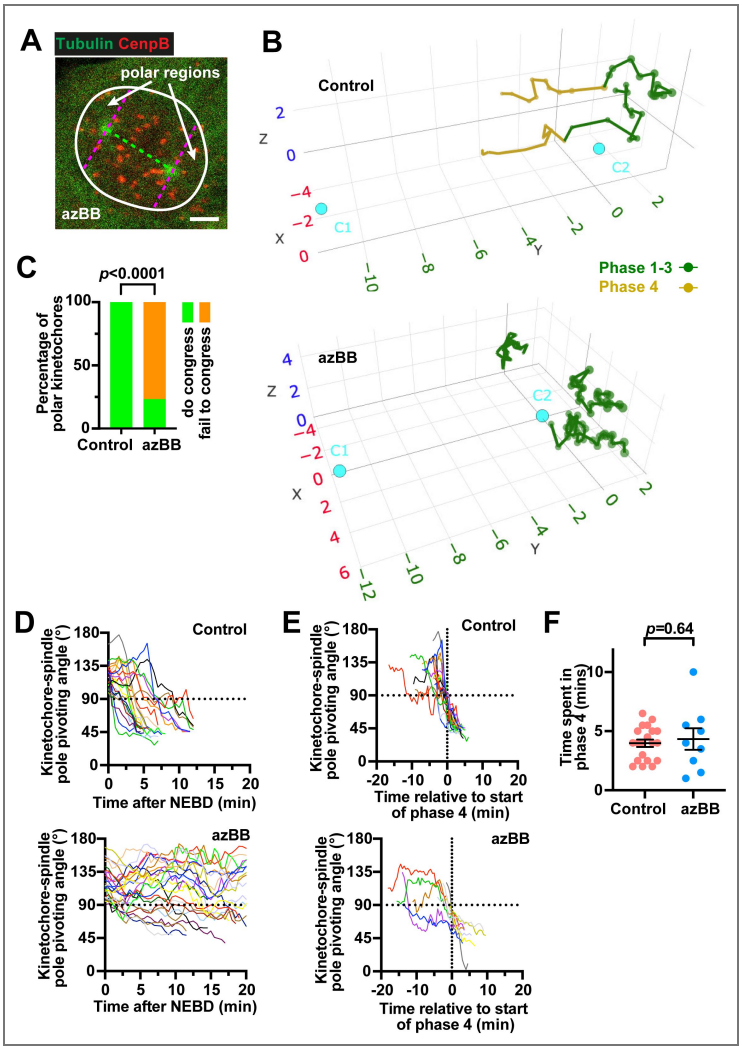

Figure 5. PANEM contraction is important to reposition kinetochores in polar regions at NEBD for efficient congression.

(A) Image of a cell in late prophase expressing CENPB-mCherry and GFP-αTubulin. The white line indicates the position of the nuclear membrane. The dotted green line is the line connecting the spindle poles. The magenta dotted lines are those on one spindle pole and perpendicular to the green dotted line. The polar regions are defined as the nuclear regions behind the pink dotted lines. Scale bar is 5μm. **(B)** The motions of representative kinetochores are shown in 3D space over time in control cells (top) or azBB-treated cells (bottom), as in Figure 3B. The colors of the kinetochore track represent Phase 1-3 (green), Phase 4 (yellow) as described in Figure 2C. The scales on all three axes are in μm. **(C)** Graph shows the percentage of polar kinetochores (at NEBD) that congressed in control (left) or azBB-treated (right) cells. The *p* values were obtained by Fisher's exact test. Number of polar kinetochores was 23 and 22 from control and azBB-treated cells, respectively. **(D)** Plots show changes in pivot angles (defined as in Figure 2A) of polar kinetochores (at NEBD) over time after NEBD (time 0), from control cells (upper panel) and azBB-treated cells (lower panel). Individual colored lines indicate individual kinetochores. The dotted line indicates the angle at which a polar kinetochore (>90°) passed into the region between the poles (central region) (<90°). The number of polar kinetochores analyzed was 23 and 25 from 5 control and 2 azBB-treated cells, respectively. Figure 5 - figure supplement 2 shows the analyses of 35 polar kinetochores from 3 individual azBB-treated cells – the data only from the first two azBB-treated cells are shown in D to avoid overcrowding in the graph. **(E)** Plots show changes in pivot angles of polar kinetochores (at NEBD) over time, as in D but aligned according to start of congressional motion (time 0). Number of polar kinetochores analyzed was 23 and 10 from 5 control and 3 azBB-treated cells, respectively. For azBB-treated cells, plots show only the polar kinetochores that subsequently exhibited congression. **(F)** Graph shows the duration of Phase 4 for polar kinetochores (at NEBD) from control (red) or from azBB-treated (blue) cells. The *p* values were obtained by t-test. Number of polar kinetochores was 20 and 9 from 5 control and 3 azBB-treated cells, respectively. For azBB-treated cells, the graph includes only the polar kinetochores that subsequently showed congression. The source data for these analyses (coordinates of kinetochores and spindle poles) can be found in Figure 5 – source data 1 and 2.

The PANEM contraction repositions chromosomes from polar regions to ensure timely congression towards the spindle mid-plane

We next analyzed the motion of kinetochores, which were localized in polar regions at NEBD (polar kinetochores) (Figure 5A). For many polar kinetochores, it was hard to discriminate Phase 1 and Phase 2 because the direction of kinetochore movement was similar between the two phases. Therefore, our analysis focused on the transition from Phase 3 to Phase 4, i.e. the start of chromosome congression towards the spindle mid-plane. In previous studies, the start of chromosome congression was identified as the most critical regulatory step to avoid the missegregation of chromosomes localizing at polar regions [18,19]. Meanwhile, it was also reported that congression of polar kinetochores to the mid-plane was facilitated by the separation of centrosomes and spindle elongation because these motions help to pivot captured polar kinetochores (those interacting with a MT emanating from one spindle pole) into the space between the two spindle poles [23]. To measure the specific effect of PANEM contraction on polar chromosomes, we investigated cells where the start of chromosome congression should be minimally affected by spindle elongation. This was possible because, in U2OS *cdk1-as* cells (that we used in this study), it had been previously shown that arrest and release at the G2-M boundary leads to most cells having a fully (or almost fully) elongated spindle at NEBD [21]. Among the cells selected in our experiments here, after NEBD, the spindle lengths were observed to gradually shorten, which occurred similarly between control and azBB-treated cells (Figure 1 – figure supplement 6).

Figure 5B shows examples of how polar kinetochores subsequently changed their positions over time after NEBD, relative to the nearest spindle pole, in control and azBB-treated cells. After identifying polar kinetochores at NEBD, we addressed whether they successfully congressed to the spindle mid-plane at later time points. While all polar kinetochores successfully congressed in control cells, 77% (23/30) of polar kinetochores failed to show congression in azBB-treated cells (Figure 5C). We then analyzed the angle between the spindle axis and the line from the kinetochore to the nearest spindle pole (Figure 2A, pivot angle): if a kinetochore was in the polar region, the angle was > 90°, and if in the region between the poles, it was < 90°. In control cells, most of the kinetochores moved from the polar region to the region between the poles (i.e. their angles became < 90°) within 10 min of NEBD (Figure 5D, control). After movement to the region between poles, congression (Phase 4) usually started soon after (Figure 5E, control). In contrast, in azBB-treated cells, the majority of polar kinetochores stayed in polar regions for 20 min (or more) after NEBD (Figure 5D, azBB, Figure 5 – figure supplement 1). A few kinetochores moved from the polar region to the region between the poles in azBB-treated cells, and in most such cases, similar to kinetochores from control cells, they showed congression soon afterwards (Figure 5E, azBB). Once congression started, kinetochores showed similar congression time, travel distance and speed in control and azBB-treated cells (Figures 5F, Figure 5 – figure supplement 2) as was the case for Phase 4 of peripheral non-polar kinetochores (Figure 4 – figure supplement 1J-L). These results suggest that the PANEM contraction facilitates movement of polar kinetochores out of polar regions and advances the onset of congression to the spindle mid-plane.

The PANEM contraction may achieve these effects by limiting the space of polar regions where polar chromosomes are located. To address this, we visualized both chromosomes and PANEM (in addition to the mitotic spindle) in control and azBB-treated cells with live-cell imaging (Figure 6A). We then quantified (1) the volume inside the PANEM at the back of a spindle pole (i.e. at the polar region) (Figure 6B) and (2) the chromosome volume present at the polar region (Figure 6C). Both volumes were rapidly reduced following NEBD in control cells, but the speed of reduction was diminished in azBB-treated cells (Figure 6B, C; Figure 6 – figure supplement 1). Thus, the polar region where polar chromosomes can be located was reduced by the PANEM contraction, which we reason facilitated their exit from the polar region.

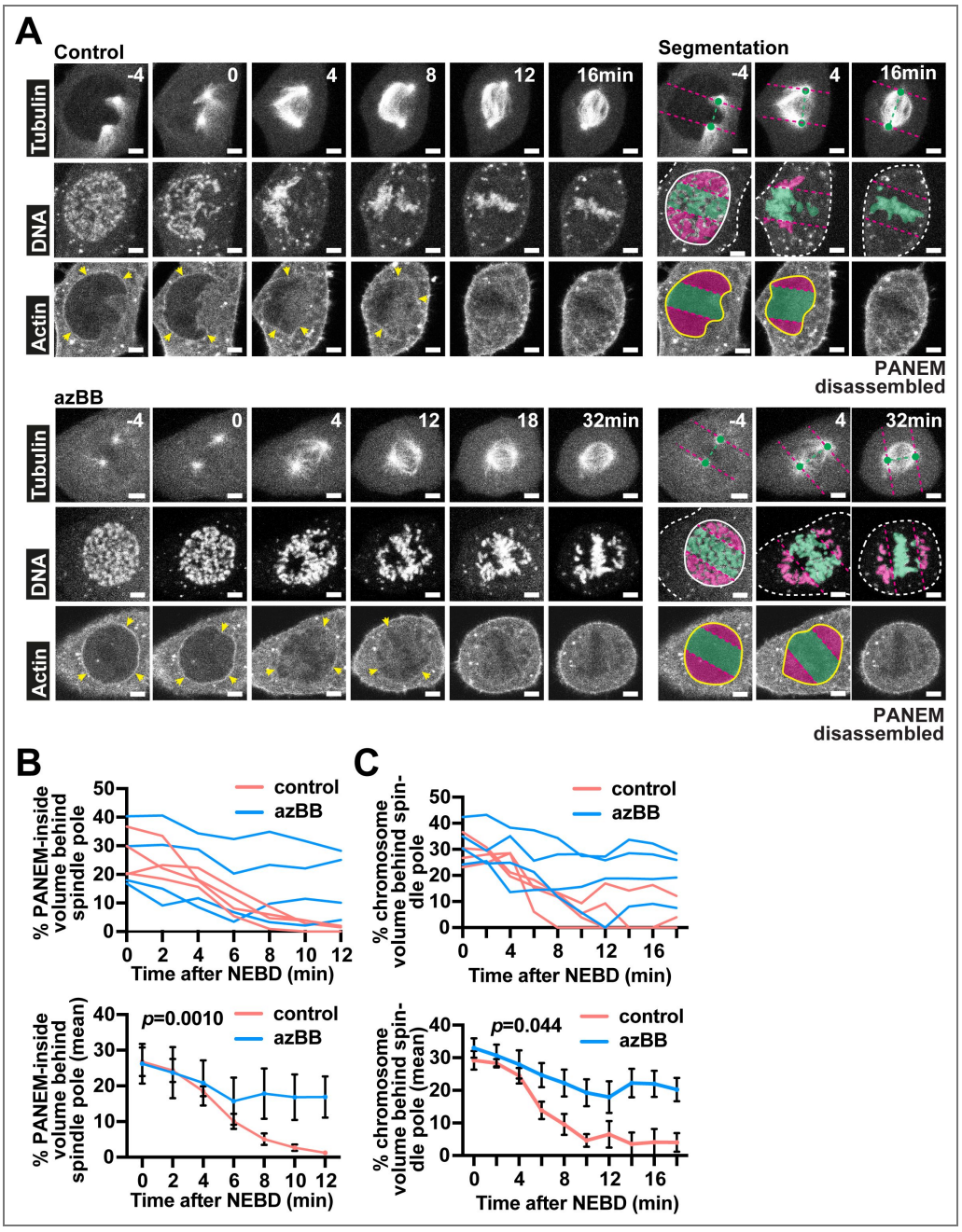

Figure 6. PANEM contraction leads to a rapid reduction of the PANEM-inside volume and chromosome volume at polar regions in early mitosis.

(A) Time-lapse images show representative cells passing through the early stages of mitosis (prophase and prometaphase). A stable cell line expressing mCherry-LifeAct and GFP-αTubulin, with chromosomes visualized by SiRDNA, were treated (or not) with azBB and were imaged every 2 minutes. Times shown were relative to NEBD. In the left-hand images the PANEM is indicated by yellow arrowheads. On the right-hand side, selected images have been reproduced to highlight segmentation. In the upper images, polar regions are designated by spindle poles (green dots) and their perpendicular planes (magenta dotted lines) (see Figure 5A). Chromosome (middle images) or PANEM (lower images) volumes behind or between the spindle poles are colored with magenta or green shading, respectively. In the middle images, solid white lines represent the cell nucleus (before NEBD) and white dotted lines represent the cell periphery. In the lower images, yellow lines represent the PANEM. Scale bars are 5μm. **(B and C)** Graphs show changes in PANEM-inside volume (B) and chromosome volume (C) behind the spindle poles as calculated for control (red lines) or azBB-treated (blue lines) cells. In the upper graph, the changes at individual polar regions are shown while in the lower graph, the change in mean is shown. The bars represent the SEM. The *p* value was obtained by t-test performed after regression analysis (see Figure 6 – figure supplement 1). In B and C, the same polar regions were analyzed.

Evidence that the contractile PANEM directly pushes both polar chromosomes and non-polar peripheral chromosomes inward

The PANEM is formed on the outer surface of the NE during prophase [20]. When the PANEM-inside volume is reduced by the PANEM contraction following NEBD, the PANEM (and the NE remnants underneath) may physically push chromosomes inwards at both polar regions and non-polar peripheral regions. To address this, we visualized both the PANEM and chromosomes (DNA) by live-cell microscopy (Figure 7A). We focused on the first 4.5 min after NEBD, during which Phase 1 was completed in most of the cells not treated with azBB (Figure 3C). We quantified the signals of PANEM and the DNA mass in selected orientations (Figure 7B) and plotted their intensities against the distance from the centre of DNA mass over time (Figure 7C). Both PANEM and the outer edge of DNA moved inward over time, at both polar and non-polar regions (Figure 7C). During this process, PANEM was always positioned at the outer edge of DNA (Figure 7D, E). We obtained similar results in more cells (Figure 7 – figure supplement 1). These data provide evidence that the contractile PANEM pushes both polar chromosomes and non-polar peripheral chromosomes inward to reposition them.

PANEM contraction helps eliminate polar chromosomes in multiple cell lines, while PANEM is absent in some chromosomally unstable cancer cells

While some cancer cell lines exhibit frequent chromosome missegregation, leading to numerical chromosomal instability (N-CIN+), and aneuploidy, other cell lines exhibit normal chromosome segregation and euploidy (N-CIN-)[29]. In our previous study, in addition to U2OS cells, we found that PANEM forms in RPE1 cells (N-CIN-) but not in HeLa cells (N-CIN+) [20]. We extended this analysis to additional human cancer cell lines (and also referred to a previous report [21]), focusing on their N-CIN status. Intriguingly, PANEM formation was observed in all four N-CIN- cell lines, but was absent during prophase in 3 out of 5 N-CIN+ cell lines (Figure 8A, Figure 8 – figure supplement 1). This suggests that the absence of PANEM in some cancer cell lines may contribute to numerical chromosomal instability.

So far, we have studied the roles of PANEM contraction in U2OS cells. In U2OS cells, PANEM contraction rapidly reduced CSV following NEBD and eliminated polar chromosomes during prometaphase and metaphase [20] (Figure 1E-G). We next addressed whether PANEM contraction plays similar roles in other cell lines that form PANEM in early mitosis. First, we inhibited PANEM contraction with myosin-II inhibitor pnBB in RPE1 cells. Similar to what we observed in U2OS cells [20], pnBB treatment slowed CSV reduction following NEBD in RPE1 cells (Figure 8B, C). In a second experiment, we arrested U2OS, RPE1, HCT116, and HeLa cells in late G2 with the Cdk1 inhibitor RO-3306, and subsequently released them into mitosis by washing out the inhibitor in the presence and absence of pnBB. With pnBB, the number of cells with polar chromosomes during metaphase increased in cell lines with PANEM (U2OS, RPE1, HCT116), but not significantly in the cell line without PANEM (HeLa) (Figure 8D, E). We conclude that the roles of PANEM in CSV reduction and in eliminating polar chromosomes are not limited to U2OS cells but are also found in other cell lines that form PANEM.

Discussion

To ensure high-fidelity chromosome segregation, kinetochore-MT interactions must be efficiently and correctly established. This process is affected by the locations of chromosomes in cells: kinetochore-MT interactions occur less efficiently for chromosomes at the nuclear periphery or behind spindle poles (polar regions), resulting in a higher risk of mis-segregation during anaphase [18,19]. The current study shows that contraction of the PANEM shortly after NEBD moves chromosomes, which were originally located at the nuclear periphery at NEBD, inward. This facilitates their kinetochores' initial interaction with spindle microtubules (Phase 1 to 2, Figure 3) and also promotes the onset of their congression towards the spindle mid-plane (Phase 3 to 4,

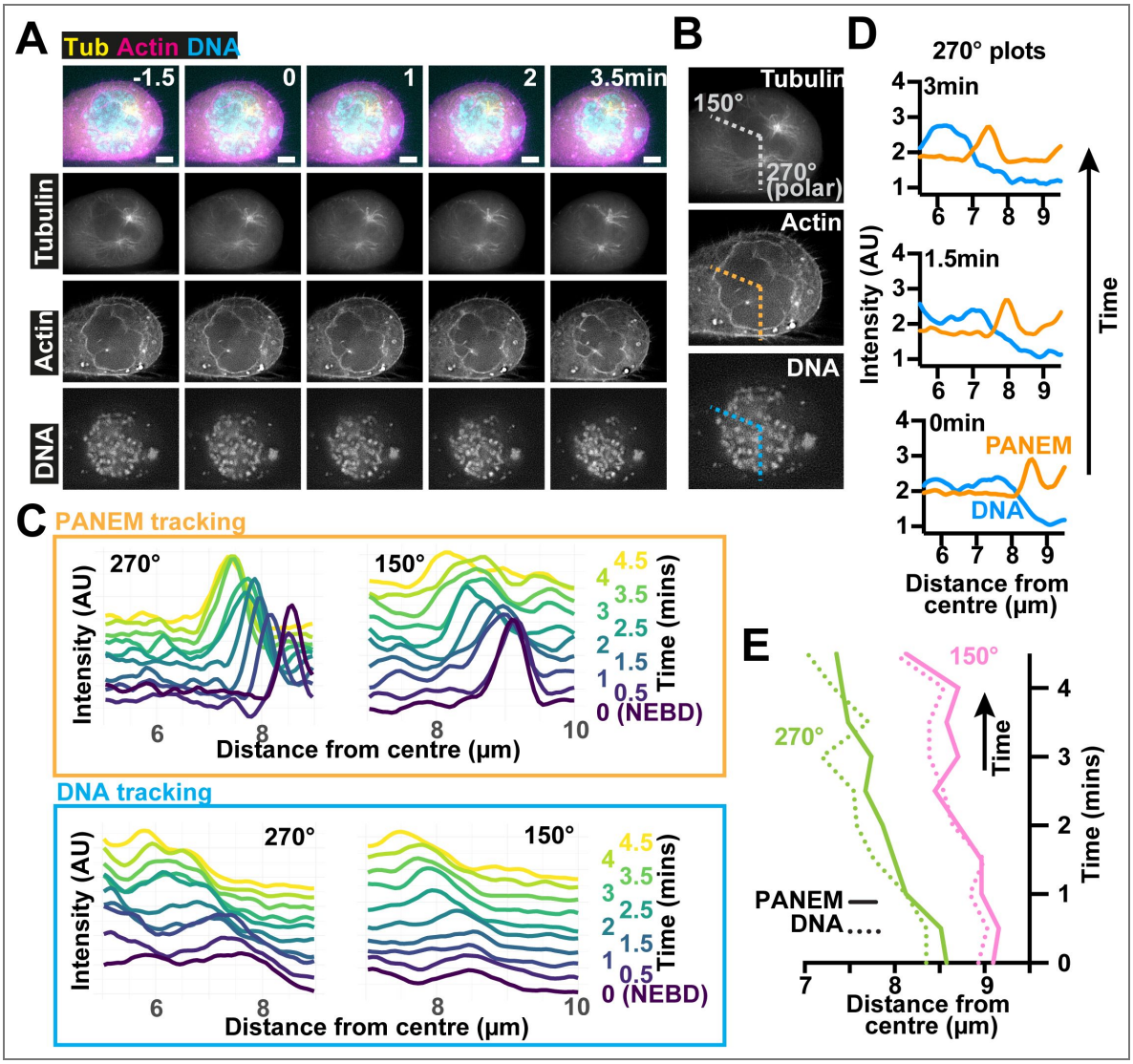

Figure 7. Evidence that the contractile PANEM directly pushes both polar chromosomes and non-polar peripheral chromosomes inward during early stages of mitosis.

(A) Time-lapse images show a representative cell passing through the early stages of mitosis (prophase and prometaphase). A stable cell line expressing mCherry-LifeAct and GFP-αTubulin, with chromosomes visualized by SYTO deep-red, were imaged every 30 seconds. NEBD is indicated at time 0. Scale bars 5μm. **(B)** Image 1.5min before NEBD from the time-lapse sequence in A to indicate the positions of line profiles. Dotted lines indicate the line profiles that pass the non-polar region (150°) and the polar region (270°) of the cell. **(C)** Graphs showing line profiles, offset in the y-axis according to time, for PANEM (upper panel; orange frame) or chromosomes (lower panel; blue frame) for the lines indicated in B. As time progresses peaks move to the left, which indicates movement closer towards the chromosome mass center. **(D)** Graphs show a time sequence of intensities calculated along the line profiles that pass the polar region of the cell shown in A. Time progresses upwards, and the colored lines indicate the intensities for Actin (PANEM; orange) or chromosomes (blue). **(E)** Graph shows the progression of the relationship between the PANEM peak and the chromosome front, over time, through the line profiles indicated in B.

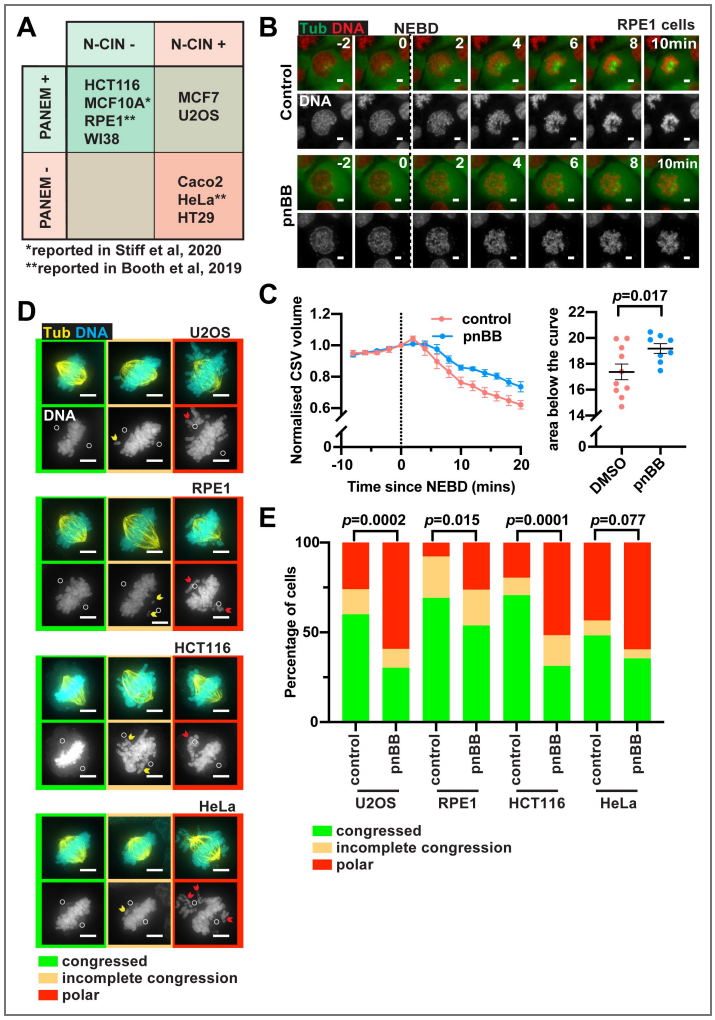

Figure 8. PANEM formation and function in non-cancer and cancer cell lines with and without numerical chromosomal instability.

(A) Cell lines from this study (the U2OS cell line primarily used in this study and five cell lines in Figure 8 – figure supplement 1), from our previous study (HeLa and RPE1 [20]), and from a study conducted by another group (MCF10A [21]) were classified according to N-CIN+ or N-CIN-, i.e. with and without numerical chromosomal instability, respectively [56]. Note that the PANEM status reported here for HCT116, RPE1 and U2OS cell lines were also confirmed by studies carried out independently of those from our lab [21]. **(B)** Time-lapse images show a representative RPE1 cell passing through the early stages of mitosis (prophase and prometaphase). A stable cell line expressing GFP-αTubulin, with chromosomes visualized by SYTO deep-red was imaged every 2 minutes after release from G2/M boundary. The timing of NEBD is indicated by the dotted line. Scale bar is 5μm. **(C)** The graph on the left shows the average change in normalized CSV for RPE1 cells imaged in B before and after NEBD (0 min) for cells treated with or without pnBB. The data from each cell was normalized to the volume at 0 minutes (immediately after NEBD) with standard error of mean (SEM) shown for each time point for each condition. The graph on the right plots the areas under the curves, measured in individual cells (which are shown in Figure 8 – figure supplement 2). The bars represent the mean and SEM. The number of cells for each group was 10 and 8 for control and pnBB, respectively. The *p* value was obtained using t-test. **(D)** Immunofluorescence of αTubulin and chromosomes (DAPI) in mitotic cells fixed 50 minutes after release from G2/M boundary. Different cell lines are shown from top to bottom, and different outcomes for each were observed, shown with coloured frames, from left to right. Those in green frames represent cells with successful alignment of all chromosomes; in orange some chromosomes had not completely aligned but were between the spindle poles (yellow arrow heads); in red some chromosomes had not aligned and remained behind the spindle poles (red arrow heads). In the lower image panels, showing DNA, for each cell line, the white circles represent the position of the spindle poles. Scale bars 5μm. **(E)** Quantification of chromosome alignment outcomes in different cell lines following treatment with DMSO (control) or pnBB for cells exemplified in D. Outcomes are shown in green, orange and red bars, as defined and using the same colors as in D. The *p* values were obtained using chi-square test for trends. The numbers of analyzed cells were 50, 76, 52, 80, 41, 64, 60 and 79 (left to right).

Figure 4). Notably, once these chromosomes initiate a poleward motion or congression (Phases 2, 4), the subsequent motions themselves are independent of PANEM contraction as might be predicted for MT-dependent motions (Figures 3 and 4). Moreover, the PANEM contraction reduces the volume of polar regions to help chromosomes escape from these regions, which allows initiation of their congression (Figures 5 and 6). The PANEM contraction seems to promote these processes by directly pushing chromosomes inward at the nuclear periphery and polar regions (Figure 7). Thus, the PANEM contraction relocates chromosomes from the regions where kinetochore-MT interactions are less efficient to regions where such interactions more readily occur (Figure 9). This ensures bi-orientation of sister chromatids and high-fidelity chromosome segregation.

In our study, we exposed the whole nucleus to infrared light to activate azBB and inhibit myosin II on the PANEM. It was technically very difficult to activate azBB only at the NE regions where the PANEM is formed. One could argue that the defective kinetochore-MT interactions with azBB treatment, found in this study, might be due to inhibition of other actomyosin networks in the nucleus (e.g. present on centrosomes or on the spindle) [30–33]. However, this is unlikely for the following reasons: (1) We did not detect any actin network inside the nucleus, on the spindle or between chromosomes in our study, at least, using the method and the cell line in the current study; (2) The inhibition of myosin II by azBB caused defective kinetochore-MT interactions for peripheral kinetochores, but not kinetochores located in central regions of the nucleus. If a possible actomyosin network in the nucleus, on the spindle or between chromosomes, were important for kinetochore-MT interaction in our system, we would expect defects for both peripheral and central kinetochores; and (3) While unconventional myosin-10 localizes at spindle poles and plays important roles in mitosis [34,35] it is unlikely to be affected in this study since, in contrast to myosin II, myosin-10 is not suppressed by blebbistatin [33], the parent myosin II inhibitor from which azBB was derived.

The PANEM contraction relocates chromosomes from polar regions and helps them initiate chromosome congression to the spindle mid-plane (Figure 5). A recent study suggested that centrosome separation and spindle elongation also play similar roles in helping chromosomes escape from polar regions and initiate congression [23,36]. We speculate that the two mechanisms might work in parallel and likely cooperate. It has been shown that spindle elongation can occur with different timings between different cell lines and between different cells of the same cell line – in some, the spindle elongation occurs before NEBD, while in others after NEBD [21,23,37]. Therefore, if spindle elongation is completed before NEBD but large polar regions remain when NEBD occurs (as we often observed in U2OS cells in the current study), the subsequent PANEM contraction would be important to eliminate the polar regions to help polar chromosomes escape from these regions. Alternatively, in cells where NEBD occurs before spindle elongation is completed, the spindle elongation and PANEM contraction could cooperate to move chromosomes out of polar regions. We intended to compare the effect of PANEM contraction in U2OS cells in which spindle elongation occurred before or after NEBD. However, we could not address this because spindle elongation usually occurred before NEBD in asynchronously growing U2OS cells, and elongation after NEBD was rare (and modest if observed; Figure 5 – figure supplement 3). In the future, it would be important to investigate how the two mechanisms – PANEM contraction and spindle elongation – cooperate to reduce polar chromosomes and under which conditions each mechanism is predominant (e.g. different cell lines, different timing of spindle elongation).

In the current study, we were able to identify kinetochore motions towards a spindle pole (Phase 2) and later, towards the spindle mid-plane (Phase 4), during prometaphase of U2OS cells (Figure 2). By contrast, a previous study, using RPE1 cells, suggested that kinetochores stayed near the spindle mid-plane and their motions towards a spindle pole and towards the spindle mid-plane were rather modest during prometaphase [5]. This difference may be explained by the different timing of spindle elongation (the increase in distance between two spindle poles): This primarily occurred before NEBD in U2OS cells, while it mainly happened after NEBD in RPE1 cells [5].

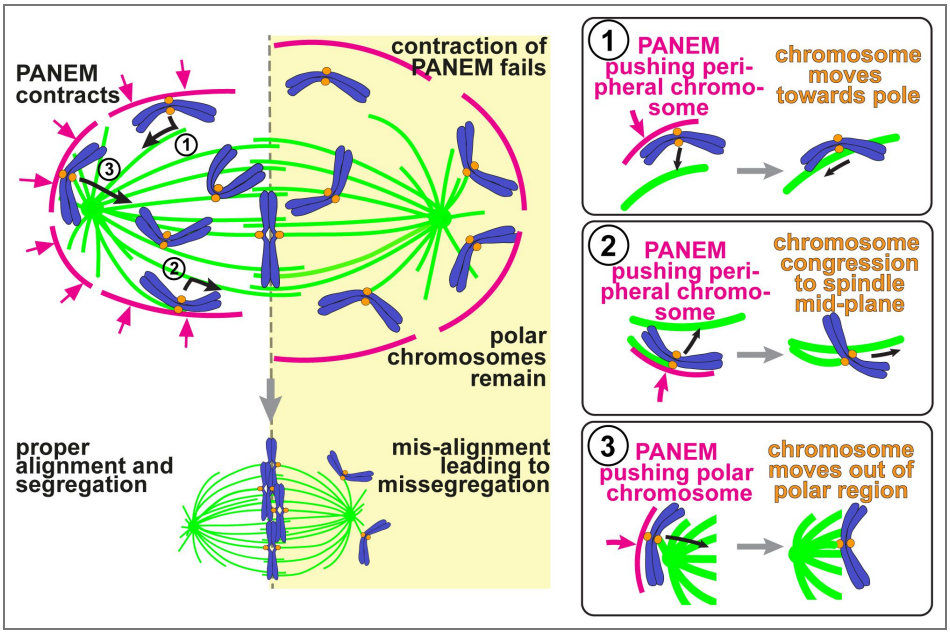

Figure 9. Model showing the effect of PANEM on peripheral/polar chromosomes.

Left-hand side shows the model of how the PANEM contraction helps to prevent chromosome misalignment and subsequent missegregation (not shown) by pushing peripheral and polar chromosomes inward so that they can be efficiently captured on spindle MTs and subsequently transported to the spindle mid-plane where they become bioriented. With reduced PANEM contraction (yellow-coloured box), chromosomes often remain in polar regions. On the right-hand side, the cartoons framed in boxes show the three main effects of PANEM contraction: (1) initial capture of a kinetochore on a peripheral chromosome by a MT, emanating from one of the spindle poles (Phase 1), so that subsequent movement towards that pole starts efficiently; (2) second MT interaction of sister kinetochore on a peripheral chromosome (Phase 3) allowing the start of congression towards the spindle mid-plane; (3) relocation of a polar chromosome to the region between the spindle poles to facilitate productive MT interactions. Figure 9 – figure supplement 1 shows an alternative model of how PANEM contraction advances the onset of chromosome congression.

It has been a widely accepted view that chromosomes congress to the spindle midplane before establishment of biorientation, whereby sister kinetochores interact with MTs from the opposite spindle poles [12]. However, very recently, this view has been challenged by a new model where biorientation precedes congression and therefore promotes it [25]. In any case, our results can be understood from both points of view. The first model (congression precedes biorientation) has been discussed in detail above. In the second model (where biorientation precedes congression), PANEM contraction could facilitate biorientation of non-polar peripheral chromosomes by constricting MTs from the spindle poles into a smaller region, thus focusing their extension towards chromosomes beyond the spindle midplane (Figure 9 – figure supplement 1). In this second situation, PANEM contraction would also facilitate biorientation of polar chromosomes by relocating them to non-polar regions with congression following [18,22,25].

Our results show that, during prophase, the PANEM is rapidly formed on the cytoplasmic side of the NE, relying on the LINC complex [20] (Figure 1A). Immediately after NEBD, the PANEM shows a rapid myosin-II-dependent contraction [20] (Figure 1C, D). Temporal regulation of the PANEM assembly and subsequent contraction should be crucial for the role of PANEM during prometaphase, which has been revealed in the current study. However, it is still unclear what triggers rapid PANEM assembly and contraction with such precise timing. PANEM assembly may be dependent on mitotic kinase activation of PANEM regulators (e.g. LINC complex [38], actin nucleators [39]). PANEM contraction may be triggered by reduced tension on the NE (triggered by NEBD [40]) or rapid accumulation of myosin-II on the perinuclear actin network [20]. In the future, uncovering the molecular mechanisms responsible for temporal regulation will help to obtain a complete picture of PANEM regulation and function in early mitosis.

Our previous study used a dominant-negative LINC construct (LINC-DN) to impair the formation of PANEM [20]. LINC-DN attenuated the reduction of CSV soon after NEBD and increased the number of polar chromosomes [20]; i.e. in this regard, the outcome was similar to azBB treatment in the current study. One might also expect that global actin polymerization inhibitors would inhibit the PANEM formation and show effects similar to LINC-DN. By contrast, it was reported that global actin polymerization inhibitors (e.g., cytochalasin D, latrunculin A) strongly affect mitotic rounding and cytokinesis but only modestly influence early chromosome movements [23,41,42]. One possibility is that such differences may have arisen from different cell types – this could be important, especially given that some cells form the PANEM and others do not (Figure 8A). A second possibility is that cytokinesis, mitotic rounding and PANEM formation may rely on actin polymerization to different extents. For example, the same concentration of global actin polymerization inhibitors may affect cytokinesis, but may still allow PANEM formation to proceed without observable effects on early chromosome movements.

It has been demonstrated that the actin network cooperates with the spindle MTs to allow high-fidelity chromosome segregation. Well-known examples are the actin network along the cell cortex, which regulates the spindle orientation and positioning [43,44], and the actomyosin ring at the cell division site, which promotes cytokinesis [45]. In addition, actin networks on/around the nucleus and within the spindle also facilitate chromosome segregation in mitosis and meiosis [46]: For example, in starfish oocytes, the actin depolymerization underneath the NE remnants facilitates chromosome interaction with spindle MTs [47,48]. In mammalian oocytes, actin dynamics on the spindle promote robust kinetochore-MT interactions and chromosome clustering to ensure chromosome segregation [49,50]. In mouse preimplantation embryos, the actin network is formed between chromosomes and its contraction due to actin disassembly helps chromosome clustering and congression [51]. In these systems, the actin network contributes to the proper positioning of chromosomes, which are widely scattered in oocytes and cells of the early embryo, to prepare for their subsequent segregation. In the present study, we describe a crucial role of a distinct actin network in repositioning chromosomes from unfavorable locations to facilitate their interaction with the mitotic spindle in human cells. These studies highlight the remarkable adaptability of actin networks in assisting the spindle MTs to safeguard faithful chromosome segregation during cell division of different cell types and across different species.

Finally, we investigated PANEM formation in N-CIN+ and N-CIN- cell lines. Intriguingly, PANEM formation was observed during prophase in all four N-CIN- cell lines, but was absent at this time in 3 out of 5 N-CIN+ cell lines (Figure 8A). These results raise two interesting possibilities. First, the absence of PANEM in some cancer cell lines may itself contribute to numerical chromosome instability. In the future, to test this possibility, a systematic study of a wider range of cancer cells and normal cells will be required. Second, cells without PANEM might have evolved compensatory mechanisms for efficiently establishing interactions between chromosomes and the spindle MTs (e.g. required for chromosome congression): For example, (1) the enhanced assembly rate of spindle MTs may facilitate kinetochore-MT interactions in N-CIN+ cancer cells [52]; (2) chromosome biorientation may precede congression more frequently to promote the congression towards the spindle midplane [25]; or (3) the balance between CENP-E, Dynein and chromokinesin's activities may incline to greater chromosome-arm ejection forces towards the spindle midplane [22]. If PANEM is widespread in normal tissues, then targeting these compensatory mechanisms could open opportunities for selectively killing PANEM-deficient cancer cells.

Materials and Methods

Cell Culture

The human cell line U2OS *cdk1-as* (male) was created by and obtained from the laboratory of Helfrid Hochegger [53]. The human cell lines MCF7 (ATCC HTB-22; female), WI38 (ATCC CCL-75; female), HT29 (ATCC HTB-38; female), HCT116 (ATCC CCL-247; male), Caco2 (ATCC HTB-37; male) and hTERT RPE1 (referred to in this manuscript as RPE1; ATCC CRL-4000; female) were all obtained from American Type Culture Collection. U2OS *cdk1-as* cells and derivative cell lines were cultured at 37°C and 5% CO2 under humidified conditions in DMEM (with L-glutamine) (Thermo Fisher; 41966-052), 10% FBS (Thermo Fisher; 10270106), 100 U/ml penicillin and 100µg/ml streptomycin (Thermo Fisher; 15140-122). For live-cell microscopy, the above medium was replaced with Fluorobrite DMEM medium (Thermo Fisher; A18967-01) supplemented with 10% FBS, 2mM L-Glutamine (Thermo Fisher; 25030-024), 1mM Sodium Pyruvate (Lonza; 13-115E) and 25 mM Hepes (Thermo Fisher; 15630080). WI38 and MCF7 cells were cultured under the same conditions as above. Caco2 cells were grown under the same conditions as above except with medium supplemented with 20% FBS. HT29 and HCT116 cells were grown under the same conditions except using McCoys 5a Medium (Thermo Fisher; 26600080) supplemented with 10% FBS. RPE1 cells were grown under the same conditions except using DMEM-F12 medium (Thermo Fisher; 31331028) supplemented with 10% FBS and 100 U/ml penicillin and 100µg/ml streptomycin. Transfection of plasmids into U2OS *cdk1-as* cells or derivative cell lines was carried out using Fugene HD (Promega; E2311) according to manufacturer guidelines. Briefly, cells were transfected in single wells of a 6-well dish using 3µl Fugene HD and 1µg plasmid (3:1 ratio). The selection agents G418 (Formedium; G418S; 300µg/ml) or Blasticidin (Invivogen; ant-bl-1; 2µg/ml) were introduced 24-48 hours after transfection.

Transfection of plasmids into RPE1 cells was carried out using the NEON Electroporation system (Thermo Fisher). For each transfection, 1 x 10^6 cells were electroporated with up to 1.5µg of plasmid DNA according to manufacturer's guidelines. Briefly, the cells were resuspended in 50µl of resuspension buffer and cells/DNA were electroporated sequentially in 10µl batches using the following conditions 1050V; 30ms width; 2 pulses. Cells were then placed immediately into 0.5ml fresh medium before being spun-down and resuspended in 2ml fresh medium in a single well of a 6-well dish. The selection agent G418 (Formedium; G418S; 500µg/ml) was introduced 24-48 hours after transfection.

U2OS *cdk1-as* (and derivative) cells expressing CDK1as were synchronized at the G2/M boundary using 1NMPP1 (Sigma; 529581-1MG). Briefly 0.2 x 10^6 cells were seeded in 2 ml of medium in 3cm glass-bottomed microscope dishes (World Precision Instruments). 16 hours before imaging 1NMPP1 was added at a final concentration of 1µM and incubated for 12 to 16 hours. 1NMPP1 was then removed and cells were washed with 10 x 1ml of fresh medium to release cells into mitosis.

In the cell lines that did not contain the *cdk1-as* allele, enrichment of cells at the G2/M boundary was achieved using the CDK1 inhibitor RO-3306 (Selleck Chemicals; S7747). Briefly, 0.2 x 10^6 cells were seeded in 2 ml of medium in 3cm glass-bottomed microscope dishes (World Precision Instruments). 6-8 hours before imaging, RO-3306 was added at a final concentration of 8μM and incubated for 6 to 8 hours. Medium containing RO-3306 was then removed and cells were washed with 10 x 1ml of fresh medium to release cells into mitosis.

The microtubule destabilizer Nocodazole (Sigma M-1404) was used at a concentration of 3.3μM and was added to the cells 1 hour before imaging. The Wee1 inhibitor MK-1775 (Selleck Chemicals; S1525) was added to cells with nocodazole or pnBB at a concentration of 0.5μM to facilitate release from G2/M arrest. The DNA stain SiR-DNA (Spirochrome/Tebubio; SC007) was used at a concentration of 100nM and was added to cells approximately 16 hours before imaging. The DNA stain SYTO-deep red (Thermo Fisher; S34900) was used at a concentration of 1μM and was added 2-3 hours before imaging. The myosin II inhibitor para-nitroBlebbistatin (pnBB; motorpharmacology/Tocris) was used at a concentration of 10-50μM and the photoactivatable Myosin II inhibitor azido-Blebbistatin (azBB; motorpharmacology) was used at a concentration of 5μM. Both of these were added to cells immediately after release from G2/M arrest (just before imaging).

Plasmid construction

For stably expressing CENPB-mCherry in G418 resistant U2OS cells the plasmid pT3570 was generated. It is a derivative of pCENPB-mCherry (Addgene 45219; a gift from the laboratory of Michael Lampson) with the G418 resistance marker removed and replaced with a Blasticidin resistance marker from ploxBlastR [54].

Cell line construction

The human cell line U2OS *cdk1-as* (mentioned above), whose endogenous CDK1 genes were disrupted and that expressed *Xenopus* CDK1as transgene, was used to generate different cell lines for microscopy experiments. A derivative of this cell line expressing GFP-αTubulin under the control of the CMV promoter, designated TT215, was created by transfecting U2OS *cdk1-as* cells with the plasmid pGFP-αTubulin (a gift from the laboratory of Jason Swedlow) and selection for G418 resistance. A second derivative of U2OS *cdk1-as* that expressed GFP-αTubulin (as above) as well as H2B-mCherry, designated TT113, was created by co-transfecting cells with pGFP-αTubulin (as above) and pH2B-mCherry (a gift from the laboratory of Jason Swedlow) and selection for G418 resistance. A third derivative of U2OS *cdk1-as* that expressed GFP-αTubulin (as above) as well as mCherry-Lifeact-7 under the control of the CMV promoter, designated TT124, was created by co-transfecting cells with pGFP-αTubulin (as above) and pmCherry-Lifeact-7 (Addgene 54491; a gift from the laboratory of Michael Davidson) and selection for G418 resistance. Finally, a derivative of TT215 (as above) expressing CENPB-mCherry under the control of the CMV promoter, designated TT230, was created by transfecting cells with the plasmid pT3570 (see above section) and selection for blasticidin resistance. A derivative of the RPE1 cell line expressing GFP-αTubulin under the control of the CMV promoter, designated TT352, was created by transfecting RPE1 cells with the plasmid pGFP-αTubulin (a gift from the laboratory of Jason Swedlow) and selection for G418 resistance. Stable cell lines used in this study were verified by Eurofin authentication service, using STR profiling.

Microscope set-up, image acquisition and deconvolution

For microscope imaging that did not require the infra-red irradiation, time-lapse, live cell images were collected at 37°C with 5% CO2 while fixed cell images were collected at 25°C using a DeltaVision ELITE microscope (Applied Precision). We used an apochromatic 100x objective lens (Olympus; numerical aperture: 1.40) or 60x objective lens (Olympus; numerical aperture: 1.42) to minimize longitudinal chromatic aberration. We also routinely checked lateral and longitudinal

chromatic aberration using 100-nm multi-color beads. We did not detect any chromatic aberration between the colors observed in the current study. For signal detection we used a sCMOS camera (PCO Edge) or a Cascade 1K EMCCD camera.

To visualize cells in early mitosis, U2OS *cdk1-as* cells and derivatives were arrested at the G2/M phase boundary, using 1NMPP1 before release into mitosis (see above). Alternatively, RPE1 (and derivatives), HCT116, U2OS (no cdk1as) and HeLa were arrested at the G2/M phase boundary, using RO-3306, before release into mitosis (see above). For visualising the chromosomes and αTubulin in TT113 cells, mCherry and GFP signals were discriminated using the dichroic DAPI/FITC/mCherry/Cy5 (52-852112-001 from API). Timelapse images, in each of these channels, were acquired through 10 z-sections separated by 2µm every 2 minutes for about 3 hours using 2×2 binning. For visualising chromosomes, actin and αTubulin in TT124 cells, SYTO-Deep red, mCherry and GFP signals were discriminated using the dichroic DAPI/FITC/mCherry/Cy5 (52-852112-001 from API). For tracking early stages of PANEM contraction, timelapse images, in each of these channels, were acquired through 20 z-sections separated by 0.5µm every 30 seconds for about 1 hour using 1×1 binning. For tracking PANEM formation and dissolution, timelapse images, in each of these channels, were acquired through 14 z-sections separated by 0.75µm every 1.5 minutes for about 1 hour using 1×1 binning. For visualising chromosomes and αTubulin in TT352 cells, SYTO-Deep red and GFP signals were discriminated using the dichroic DAPI/FITC/mCherry/Cy5 (52-852112-001 from API). To track changes to CSV in such cells as they entered mitosis, timelapse images, in each of these channels, were acquired through 12 z-sections separated by 1.5µm every 5 minutes using 4×4 binning and a 60× objective.

To visualize chromosomes and actin in PFA fixed cells (various cell lines) Hoechst and phalloidin DyLight 650 signals were discriminated using the dichroic DAPI/FITC/mCherry/Cy5 (52-852112-001 from API). To visualize αTubulin and DAPI in PFA fixed immunostained cells, DAPI signal and the secondary antibody label Alexa488 were discriminated using the dichroic DAPI/FITC/TRITC/Cy5 (52-852111-001 from API). Images were acquired through 25 z-sections of 0.5µm.

After acquisition, all images were deconvolved before analysis using softWoRx software with enhanced ratio and 10 iterations. Analysis of individual cells was performed using Imaris software (Bitplane) or ImageJ [55].

For experiments that used azBB treatment that required photoactivation a Zeiss confocal 710 system with 63x objective lens (NA 1.4) was used. For photoactivation of azBB a coherent Chameleon multiphoton laser was used. AzBB photoactivation experiments were carried out in cells either expressing GFP-αTubulin and CenpB-mCherry or GFP-αTubulin and mCherry-LifeAct. In both cell lines chromosomes were stained with SiRDNA. To focus on early mitotic cells, before NEBD, prophase cells were identified and selected as those with an intact nucleus displaying early signs of chromosome condensation (note that they were confirmed later in the experiment as mitotic when NEBD was observed). After identification of a suitable candidate, a zoom factor of approximately 6x was applied to include only the nucleus of the selected cell in the field of view. A reference image was taken to visualise αTubulin, kinetochores and chromosomes or αTubulin, actin and chromosomes by scanning with 488nm, 543nm and 633nm lasers in three z-sections 2µm apart for this xy region. At the same time the nuclear region was irradiated with an 860nm Chameleon multiphoton laser to activate azBB to allow its covalent binding to Myosin II. For tracking kinetochore motions, timelapse images were then acquired of the selected cell by scanning with only 488nm, 543nm and 633nm lasers in 11-15 z-sections 1.0µm apart with a pixel size of 0.085µm every 30 seconds for approximately 20-30 minutes. For measuring volume behind the spindle poles timelapse images were then acquired of the selected cell by scanning with only 488nm, 543nm and 633nm lasers in 11-15 z-sections 1.7µm apart with a pixel size of 0.128µm every 2 minutes for approximately 40-60 minutes.

After acquisition, analysis of individual cells was performed using Imaris software (Bitplane). Unless otherwise stated, for presenting images in figures, Actin was shown as a single z slice at the sharpest focal plane (where the PANEM contour was the clearest). For DNA and αTubulin, images were of several projected z slices to convey the features of the whole nucleus or cell.

Cell fixation for visualization of chromosomes and actin or MTs

For fixed-cell visualization, cells were grown in 3cm fluorodishes (WPI) and washed once with 2ml phosphate-buffered saline (PBS) which was then replace with 2ml 4% paraformaldehyde (PFA) in PBS for 10 minutes. The cells were then washed with 2ml PBS three times. PFA fixed cells were permeabilized by treatment with 2ml room temperature PBS containing 0.5% Triton for 10 minutes. The cells were then washed with 2ml PBS twice. For visualisation of chromosomes and actin, these cells were incubated with 0.5µg/ml Hoechst 33342 (Sigma-Aldrich 14533) and 0.002 Units/µl phalloidin DyLight650 (Cell Signalling Technology; 12956) in 2ml of PBS with 5% bovine serum albumin (BSA) overnight at 4°C. Finally, cells were washed with 2ml PBS with 5% BSA then covered with 2ml PBS and imaged immediately.

For visualisation of chromosomes and MTs, immunofluorescence was carried out. After fixation (as described above) these cells were incubated with PBS containing 3% BSA at 4°C for at least 2 hours. Antibody against αTubulin (Merck; mab1864) was diluted 1:1,000 in PBS containing 3% BSA and incubated with fixed cells overnight at 4°C. The cells were then washed with 2ml PBS containing 0.1% Triton three times before incubation with the secondary antibody Donkey anti-Rat Alexa488 (Invitrogen; A21208) that was diluted 1:1000 in PBS containing 3% BSA overnight in the dark at 4°C. The cells were then washed with 2ml PBS containing 0.1% Triton three times before 20µl Prolong Gold Antifade containing DAPI (Thermo Fisher; P36935) was mounted on cells, which were sealed with coverslips.

Measuring chromosome scattering volume

Measurement of chromosome scattering volume (CSV) was carried out by a semi-automatic detection of chromosomes using Imaris (Version 8.0) software Surface tool, as described previously [20]. Contours of chromosomes on each acquired Z-section were selected, excluding any background non-chromosome signal. Imaris then generated 3D objects, representing chromosomes surface for each time point, from the selected contours. An extension script, created for Imaris in MatLab, was used to calculate the minimum polyhedron to envelope the 3D surface (also known as a convex hull), the volume of which is the CSV (see also Figure 1B).

Measuring changes in the volume inside PANEM

The analysis of the volume inside PANEM was carried out using Imaris (Version 8.0) software surface tool. Contours of the PANEM were drawn in each z-stack where the PANEM was visible as a full ring. Stacks where PANEM was indistinguishable from the actin network at the cell cortex were excluded. If the PANEM ring was detected in multiple z-stacks in a single timepoint, an average of the volume measurement in the z-stacks was taken to analyze the network contraction.

Tracking and analysis of kinetochore motions

Cells were imaged with high temporal and spatial resolution, allowing tracking of kinetochores through time (see above). Tracking was carried out by automatic identification of kinetochores using Imaris software (Version 9.5), with user supervision and occasional correction. Using this feature, x, y, z coordinates of the centre of mass of the kinetochores and centrosomes, visualized throughout prometaphase, were determined.

To understand the motions of the individual kinetochores through time, using the xyz coordinates for the different objects, the distance between the kinetochore and 3 fixed cellular points, were calculated (see also Figure 2A): (1) the spindle pole towards which the kinetochore moved after NEBD (usually the spindle pole that was closest to the kinetochore at NEBD); (2) the mid-point between the two spindle poles; (3) the shortest distance to the cell mid-plane (or metaphase plate). By setting these reference points on the spindle, we were able to analyze kinetochore motions without being affected by the motions of the spindle.

To easily visualise and clearly represent these kinetochore motions in relation to the spindle poles, a further round of processing was carried out using a python script. In brief, this script transformed the xyz coordinates of the spindle poles of a given sequence so that at each time point

the closest spindle to the kinetochore at NEBD will locate at x=0, y=0, z=0, in addition the other spindle pole will always lie at x=0, z=0 (with variable y). According to how much the spindle pole positions had rotated or shifted, the kinetochore coordinates at each timepoint were transformed accordingly such that spindle pole motions were cancelled out. R studio was used to display these corrected data on a three-dimensional plot.

We assigned phases of kinetochore motions as follows: To define Phase 2, we looked at the changes in distances of the kinetochore from the nearest centrosome. When the distance dropped in 5 consecutive timepoints (or distance dropped more than 2 μm over the course of up to 5 timepoints), we recognised this as part of Phase 2. The start was then defined as the first moment the drop in distance began (after a period of no overall change, or of increasing distance change). In some cases, when distance to the nearest pole was already gradually dropping, we assigned the start of Phase 2 at the point where there was 2 to 4-fold increase in rate, which was usually also concomitant with an increase of the kinetochores' distance from the mid-plane. When these distances changes were not clear, where it was possible, we assigned the start of Phase 2 according to the first time point we observed the overlap of the kinetochore signal with microtubules and subsequent movement towards the pole. The end of Phase 2 was assigned when the distance between the kinetochore and the nearest pole stopped shortening or began to rise slightly.

For non-polar kinetochores, the start of Phase 4 was assigned by looking for the time where the distance to the mid-plane began to decrease; usually, this was concomitant with an increase in distance from the nearest pole. The end of Phase 4 was assigned as a time when the kinetochore started oscillation (i.e. a backward motion towards a spindle pole) around the spindle mid-plane. In some cases where the kinetochore became close to the mid-plane (< 2.5 μm), it was not possible to track it further due to kinetochore crowding around the spindle mid-plane – in such cases, the end of Phase 4 was assigned as the end of tracking. For polar kinetochores, the above definition of the start of Phase 4 did not suit because the distance to the mid-plane already began to decrease before they entered the non-polar region. We therefore first specified the end of Phase 4 in the same way as above. We then looked at the corrected 3D plots of each kinetochore track (described in Materials and Methods above) and we traced the kinetochore track backwards, from the end point. We judged the start of Phase 4 for polar kinetochores as the first point that the kinetochore changed direction onto its final trajectory, of typically 4 or more consecutive timepoints, towards the mid-plane (congressional motion) after the kinetochore had passed into the region between the spindle poles.

We selected kinetochores that can be individually tracked. If kinetochore tracking was difficult because of kinetochore crowding (except towards the end of Phase 4; see above), we did not choose this kinetochore for further analyses. We also did not include kinetochores close to spindle poles (< 4 μm) at NEBD in our analysis for the following two reasons: First, these kinetochores often did not show clear and rapid movements towards a spindle pole, which we used to define Phase 2. Second, although we referred to kinetochore co-localization with a MT signal for the start of Phase 2, this was difficult for kinetochores close to spindle poles because of a high density of MTs. With such selection, all selected kinetochores without azBB treatment (control) showed the poleward motion (Phase 2) and congression (Phase 4) in this order, though their extents were varied among kinetochores. All selected kinetochores with azBB treatment also showed the poleward motion (Phase 2), and some of them showed congression (Phase 4) after Phase 2. Then, Phase 1 and Phase 3 were defined as intervals between NEBD and Phase 2 and between Phase 2 and Phase 4, respectively. If no Phase 4 was observed with azBB, we judged that Phase 3 continued until the end of tracking.

Measuring PANEM and chromosome volumes behind the spindle poles

To determine the percentage of the PANEM volume lying behind the spindle poles, and to track changes of the volume through time, the following method was developed in Imaris: First, the x, y, z coordinates of the centre of mass of spindle pole positions were determined automatically for each timepoint. Second, the PANEM volume or the chromosome volumes were determined for

each timepoint. The PANEM volume was defined using the surface tool. Contours of the PANEM were drawn in each z-stack where the PANEM was visible as a full ring, stacks where the PANEM was indistinguishable from the actin network at the cell cortex were excluded. Finally, the volumes in each z-stack were unified to create a single surface object. The chromosome volume was defined by automatic detection using the surface tool. Background signals that were outside the nucleus before NEBD were excluded. For later stages of mitosis, when chromosomes became visible as individual units, all the chromosome volumes were unified as one surface item.

After the relevant objects of the cell had been tracked an extension script, created for Imaris in MatLab, was used to cut the surface objects of the PANEM or chromosomes into three surface objects. The regions were defined by taking the line joining the spindle poles and creating perpendicular planes to this line at each pole. Surfaces were then cut, along these planes, into up to three objects. They were either between the poles (i.e. between these planes), or behind one of the poles (not between the planes). For PANEM volumes, whose surface shape was simple, the split volumes at each time point were obtained directly. For chromosome volumes, whose surface shape was more complex, the surface cut script gave a simplified chromosome surface output. To calculate the chromosome volumes in each region accurately a further round of chromosome surface tracking was performed, using the same parameters as used originally, using the individual cut surfaces as a mask.

While the above analysis was carried out in 3D (includes all z stacks) for representation of the images in Figure 6A, a projection of several z-stacks was shown for the spindle poles and a single z slice was shown for both Actin and DNA images. Note that only polar regions with >20% total chromosome volume behind the spindle at NEBD were analyzed so that potential effects on the volume reduction due to PANEM contraction can be readily detected if present. For statistical analyses, Prism was used to fit linear regression lines for the data from each pole. For the PANEM volumes, regression was calculated for the first 12 minutes. For the DNA volumes, regression was calculated for the first 20 minutes. If zero % volume was reached and persisted for 2 or more timepoints in these analyses, the remaining points after the first zero were removed before regression was calculated.

Tracking chromosome and PANEM motions using line plot profiles

We used both Imaris and ImageJ to track chromosome and PANEM movements, over time, relative to the centre of the nucleus. First, the chromosome volume and its central x, y, z coordinates were defined by automatic detection using the surface tool in Imaris at each timepoint. ImageJ was then used to plot lines, arranged radially, from the chromosome centre coordinates for each channel and timepoint using these coordinates. Intensity values along the length of each line were obtained. In some cases, where the selected centre point displayed a poorly focused PANEM, images corresponding to plus or minus 1 z-stack were used for quantification, and these were matched between channels. Subsequently, for each selected line, data were normalized by dividing by the smallest intensity value found on that line and fluorescence intensity data were smoothed by averaging across 5 consecutive data points. The PANEM peak was determined as the point of highest fluorescence intensity. The DNA front was defined as the point halfway between the peak (defined as the last point of increasing intensity following at least three consecutive points of increase) and trough (defined as the last point of decreasing intensity following at least three consecutive points of decrease). For representation of the images in Figure 7A a projection of several z-stacks was shown for the spindle poles while a single z slice was shown for both Actin and DNA images.

Statistical analysis and presentation

Graphs and statistical analyses were created and performed using Graphpad Prism (versions 7-10) and R studio (version 2024.12). All experiments were carried out at least twice and found to give consistent results. Number of cells analyzed, or data points included and the statistical tests used for each analyses are indicated in the Figure legends. The null hypotheses in statistical tests were

that the samples were collected randomly and independently from the same population. All *p* values were two-tailed, and the null hypotheses were reasonably discarded when *p* values were smaller than 0.05.

Data availability

Figures and supplemental figures contain numerical data in graphs. Sample numbers are stated in figure legends.

Acknowledgements

We thank Tanaka lab members, K. Weijer, A. Saurin and M. McLean for discussion; Dundee Imaging Facility for help with microscopy; and H. Hochegger, M. Lampson, J. Swedlow, J. Buerstedde and M. Davidson for reagents. This work was supported by the Wellcome Trust Investigator Award (219418/Z/19/Z), the Cunningham Trust PhD scholarship (CT19-06) and the Wellcome Trust Technology Platform (097945/B/11/Z). For open access, the authors will apply a Creative Commons Attribution (CC BY) license to any author-accepted manuscript version arising from this manuscript.

Additional information

Author contributions

Conceptualization: T.U.T., N.S. and J.K.E.; methodology: N.S., J.K.E., Z.Y. and A.J.R.B.; investigation: N.S. and J.K.E.; formal analysis: N.S., J.K.E. and T.U.T., software: G.B. and J.K.E.; visualization: N.S. J.K.E. and T.U.T., writing – original draft: T.U.T., N.S, and J.K.E.; writing – review and editing: T.U.T. and J.K.E.: project administration, supervision and funding acquisition: T.U.T.

Funding

Funder	Grant reference number	Author
Wellcome Trust (WT)	https://doi.org/10.35802/219418	Tomoyuki U Tanaka
Cunningham Trust	CT19-06 [PhD scholarship]	Tomoyuki U Tanaka
Wellcome Trust (WT)	https://doi.org/10.35802/097945	Tomoyuki U Tanaka

Author ORCID iDs

John K Eykelenboom: https://orcid.org/0000-0003-4115-9686
Graeme Ball: https://orcid.org/0000-0002-6526-2306
Tomoyuki U Tanaka: https://orcid.org/0000-0002-9886-5947

Author notes

Nooshin Sheidaei: Present address: Division of Cell and Molecular Biology, The Institute of Cancer Research, London, United Kingdom
Alexander JR Booth: Present address: Image Solution IMSOL, Preston, United Kingdom
Nooshin Sheidaei, John K Eykelenboom: These authors contributed equally.
Competing interests: One of the authors, A.J.R. Booth, is currently employed by IMSOL, providing service and maintenance of the DeltaVision Elite microscope used in this work. The microscope was also originally purchased through IMSOL.

Additional files

Response to Reviewers

Figure supplements

Source data legends

Figure 5 - source data 1
Figure 5 - source data 2
Figure 3 - source data 1
Figure 3 - source data 2
Figure 3 - source data 4
Figure 3 - source data 3

References

1. **Kapoor T.M** (2017) Metaphase Spindle Assembly. *Biology* **6** https://doi.org/10.3390/biology6010008 | PubMed
2. **Santaguida S.,** Musacchio A (2009) The life and miracles of kinetochores. *The EMBO journal* **28**:2511-2531 https://doi.org/10.1038/emboj.2009.173 | PubMed
3. **Hinshaw S.M.,** Harrison S.C (2018) Kinetochore Function from the Bottom Up. *Trends Cell Biol* **28**:22-33 https://doi.org/10.1016/j.tcb.2017.09.002 | PubMed
4. **Musacchio A.,** Desai A (2017) A Molecular View of Kinetochore Assembly and Function. *Biology* **6** https://doi.org/10.3390/biology6010005 | PubMed
5. **Magidson V.,** O'Connell C.B., Loncarek J., Paul R., Mogilner A., Khodjakov A (2011) The spatial arrangement of chromosomes during prometaphase facilitates spindle assembly. *Cell* **146**:555-567 https://doi.org/10.1016/j.cell.2011.07.012 | PubMed
6. **Tanaka T.U.,** Zhang T (2022) SWAP, SWITCH, and STABILIZE: Mechanisms of Kinetochore-Microtubule Error Correction. *Cells* **11** https://doi.org/10.3390/cells11091462 | PubMed
7. **Rieder C.L.,** Alexander S.P (1990) Kinetochores are transported poleward along a single astral microtubule during chromosome attachment to the spindle in newt lung cells. *The Journal of cell biology* **110**:81-95 https://doi.org/10.1083/jcb.110.1.81 | PubMed
8. **Tanaka K.,** Kitamura E., Kitamura Y., Tanaka T.U (2007) Molecular mechanisms of microtubule-dependent kinetochore transport toward spindle poles. *The Journal of cell biology* **178**:269-281 https://doi.org/10.1083/jcb.200702141 | PubMed
9. **Tanaka K.,** Mukae N., Dewar H., van Breugel M., James E.K., Prescott A.R., Antony C., Tanaka T.U (2005) Molecular mechanisms of kinetochore capture by spindle microtubules. *Nature* **434**:987-994 https://doi.org/10.1038/nature03483 | PubMed
10. **Shrestha R.L.,** Draviam V.M (2013) Lateral to end-on conversion of chromosome-microtubule attachment requires kinesins CENP-E and MCAK. *Curr Biol* **23**:1514-1526 https://doi.org/10.1016/j.cub.2013.06.040 | PubMed
11. **Itoh G.,** Ikeda M., Iemura K., Amin M.A., Kuriyama S., Tanaka M., Mizuno N., Osakada H., Haraguchi T., Tanaka K (2018) Lateral attachment of kinetochores to microtubules is enriched in prometaphase rosette and facilitates chromosome alignment and bi-orientation establishment. *Scientific reports* **8** https://doi.org/10.1038/s41598-018-22164-5 | PubMed
12. **Kapoor T.M.,** Lampson M.A., Hergert P., Cameron L., Cimini D., Salmon E.D., McEwen B.F., Khodjakov A (2006) Chromosomes can congress to the metaphase plate before biorientation. *Science* **311**:388-391 https://doi.org/10.1126/science.1122142 | PubMed
13. **Maiato H.,** Gomes A.M., Sousa F., Barisic M (2017) Mechanisms of Chromosome Congression during Mitosis. *Biology* **6** https://doi.org/10.3390/biology6010013 | PubMed
14. **Godek K.M.,** Kabeche L., Compton D.A (2015) Regulation of kinetochore-microtubule attachments through homeostatic control during mitosis. *Nature reviews. Molecular cell biology* **16**:57-64 https://doi.org/10.1038/nrm3916 | PubMed
15. **Armond J.W.,** Harry E.F., McAinsh A.D., Burroughs N.J (2015) Inferring the Forces Controlling Metaphase Kinetochore Oscillations by Reverse Engineering System Dynamics. *PLoS Comput Biol* **11**:e1004607 https://doi.org/10.1371/journal.pcbi.1004607 | PubMed

16. **Jaqaman K.,** King E.M., Amaro A.C., Winter J.R., Dorn J.F., Elliott H.L., McHedlishvili N., McClelland S.E., Porter I.M., Posch M., *et al.* (2010) Kinetochore alignment within the metaphase plate is regulated by centromere stiffness and microtubule depolymerases. *The Journal of cell biology* **188**:665-679 https://doi.org/10.1083/jcb.200909005 | PubMed

17. **Skibbens R.V.,** Skeen V.P., Salmon E.D (1993) Directional instability of kinetochore motility during chromosome congression and segregation in mitotic newt lung cells: a push-pull mechanism. *The Journal of cell biology* **122**:859-875 https://doi.org/10.1083/jcb.122.4.859 | PubMed

18. **Vukusic K.,** Tolic I.M (2022) Polar Chromosomes-Challenges of a Risky Path. *Cells* **11** https://doi.org/10.3390/cells11091531 | PubMed

19. **Klaasen S.J.,** Truong M.A., van Jaarsveld R.H., Koprivec I., Stimac V., de Vries S.G., Risteski P., Kodba S., Vukusic K., de Luca K.L., *et al.* (2022) Nuclear chromosome locations dictate segregation error frequencies. *Nature* **607**:604-609 https://doi.org/10.1038/s41586-022-04938-0 | PubMed

20. **Booth A.J.R.,** Yue Z., Eykelenboom J.K., Stiff T., Luxton G.W.G., Hochegger H., Tanaka T.U (2019) Contractile acto-myosin network on nuclear envelope remnants positions human chromosomes for mitosis. *eLife* **8** https://doi.org/10.7554/eLife.46902 | PubMed

21. **Stiff T.,** Echegaray-Iturra F.R., Pink H.J., Herbert A., Reyes-Aldasoro C.C., Hochegger H (2020) Prophase-Specific Perinuclear Actin Coordinates Centrosome Separation and Positioning to Ensure Accurate Chromosome Segregation. *Cell reports* **31** https://doi.org/10.1016/j.celrep.2020.107681 | PubMed

22. **Barisic M.,** Aguiar P., Geley S., Maiato H (2014) Kinetochore motors drive congression of peripheral polar chromosomes by overcoming random arm-ejection forces. *Nature cell biology* **16**:1249-1256 https://doi.org/10.1038/ncb3060 | PubMed

23. **Koprivec I.,** Stimac V., Dura M., Vukusic K., Mikec P., Tolic I.M (2026) Polar chromosomes are rescued from missegregation by spindle elongation-driven microtubule pivoting. *Nature communications* **17** https://doi.org/10.1038/s41467-026-69830-1 | PubMed

24. **Renda F.,** Miles C., Tikhonenko I., Fisher R., Carlini L., Kapoor T.M., Mogilner A., Khodjakov A (2022) Non-centrosomal microtubules at kinetochores promote rapid chromosome biorientation during mitosis in human cells. *Current biology : CB* **32**:1049-1063.e1044. https://doi.org/10.1016/j.cub.2022.01.013 | PubMed

25. **Vukusic K.,** Tolic I.M (2025) CENP-E initiates chromosome congression by opposing Aurora kinases to promote end-on attachments. *Nature communications* **16** https://doi.org/10.1038/s41467-025-64148-w | PubMed

26. **Kepiro M.,** Varkuti B.H., Bodor A., Hegyi G., Drahos L., Kovacs M., Malnasi-Csizmadia A (2012) Azidoblebbistatin, a photoreactive myosin inhibitor. *Proceedings of the National Academy of Sciences of the United States of America* **109**:9402-9407 https://doi.org/10.1073/pnas.1202786109 | PubMed

27. **Képiró M.,** Várkuti B.H., Rauscher A.A., Kellermayer M.S.Z., Varga M., Málnási-Csizmadia A (2015) Molecular Tattoo: Subcellular Confinement of Drug Effects. *Chemistry & Biology* **22**:548-558 https://doi.org/10.1016/j.chembiol.2015.03.013 | PubMed

28. **Taubenberger A.V.,** Baum B., Matthews H.K (2020) The Mechanics of Mitotic Cell Rounding. *Front Cell Dev Biol* **8** https://doi.org/10.3389/fcell.2020.00687 | PubMed

29. **Devillers R.,** Dos Santos A., Destombes Q., Laplante M., Elowe S (2024) Recent insights into the causes and consequences of chromosome mis-segregation. *Oncogene* **43**:3139-3150 https://doi.org/10.1038/s41388-024-03163-5 | PubMed

30. **Aquino-Perez C.,** Safaralizade M., Podhajecky R., Wang H., Lansky Z., Grosse R., Macurek L (2024) FAM110A promotes mitotic spindle formation by linking microtubules with actin cytoskeleton. *Proceedings of the National Academy of Sciences of the United States of America* **121**:e2321647121 https://doi.org/10.1073/pnas.2321647121 | PubMed

31. **Kita A.M.,** Swider Z.T., Erofeev I., Halloran M.C., Goryachev A.B., Bement W.M (2019) Spindle-F-actin interactions in mitotic spindles in an intact vertebrate epithelium. *Molecular biology of the cell* **30**:1645-1654 https://doi.org/10.1091/mbc.E19-02-0126 | PubMed

32. **Plessner M.,** Knerr J., Grosse R (2019) Centrosomal Actin Assembly Is Required for Proper Mitotic Spindle Formation and Chromosome Congression. *iScience* **15**:274-281 https://doi.org/10.1016/j.isci.2019.04.022 | PubMed

33. **Limouze J.,** Straight A.F., Mitchison T., Sellers J.R (2004) Specificity of blebbistatin, an inhibitor of myosin II. *J Muscle Res Cell Motil* **25**:337-341 https://doi.org/10.1007/s10974-004-6060-7 | PubMed

34. **Mayca Pozo F.,** Geng X., Miyagi M., Amin A.L., Huang A.Y., Zhang Y (2023) MYO10 regulates genome stability and cancer inflammation through mediating mitosis. *Cell reports* **42** https://doi.org/10.1016/j.celrep.2023.112531 | PubMed

35. **Woolner S.,** O'Brien L.L., Wiese C., Bement W.M (2008) Myosin-10 and actin filaments are essential for mitotic spindle function. *The Journal of cell biology* **182**:77-88 https://doi.org/10.1083/jcb.200804062 | PubMed

36. **Koprivec I.,** Štimac V., Mikec P., Tolić I.M (2024) Microtubule pivoting driven by spindle elongation rescues polar chromosomes to ensure faithful mitosis. *bioRxiv* https://doi.org/10.1101/2024.06.16.599200

37. **Kaseda K.,** McAinsh A.D., Cross R.A (2012) Dual pathway spindle assembly increases both the speed and the fidelity of mitosis. *Biol Open* **1**:12-18 https://doi.org/10.1242/bio.2011012 | PubMed

38. **Lombardi M.L.,** Lammerding J (2011) Keeping the LINC: the importance of nucleocytoskeletal coupling in intracellular force transmission and cellular function. *Biochem Soc Trans* **39**:1729-1734 https://doi.org/10.1042/BST20110686 | PubMed

39. **Firat-Karalar E.N.,** Welch M.D (2011) New mechanisms and functions of actin nucleation. *Current opinion in cell biology* **23**:4-13 https://doi.org/10.1016/j.ceb.2010.10.007 | PubMed

40. **Beaudouin J.,** Gerlich D., Daigle N., Eils R., Ellenberg J (2002) Nuclear envelope breakdown proceeds by microtubule-induced tearing of the lamina. *Cell* **108**:83-96 https://doi.org/10.1016/s0092-8674(01)00627-4 | PubMed

41. **Dewey E.B.,** Johnston C.A (2017) Diverse mitotic functions of the cytoskeletal cross-linking protein Shortstop suggest a role in Dynein/Dynactin activity. *Molecular biology of the cell* **28**:2555-2568 https://doi.org/10.1091/mbc.E17-04-0219 | PubMed

42. **Lancaster O.M.,** Le Berre M., Dimitracopoulos A., Bonazzi D., Zlotek-Zlotkiewicz E., Picone R., Duke T., Piel M., Baum B (2013) Mitotic rounding alters cell geometry to ensure efficient bipolar spindle formation. *Developmental cell* **25**:270-283 https://doi.org/10.1016/j.devcel.2013.03.014 | PubMed

43. **di Pietro F.,** Echard A., Morin X (2016) Regulation of mitotic spindle orientation: an integrated view. *EMBO Rep* **17**:1106-1130 https://doi.org/10.15252/embr.201642292 | PubMed

44. **Kunda P.,** Baum B (2009) The actin cytoskeleton in spindle assembly and positioning. *Trends Cell Biol* **19**:174-179 https://doi.org/10.1016/j.tcb.2009.01.006 | PubMed

45. **Pollard T.D.,** O'Shaughnessy B (2019) Molecular Mechanism of Cytokinesis. *Annual review of biochemistry* **88**:661-689 https://doi.org/10.1146/annurev-biochem-062917-012530 | PubMed

46. **Davidson P.M.,** Cadot B (2021) Actin on and around the Nucleus. *Trends Cell Biol* **31**:211-223 https://doi.org/10.1016/j.tcb.2020.11.009 | PubMed

47. **Burdyniuk M.,** Callegari A., Mori M., Nédélec F., Lénárt P (2018) F-Actin nucleated on chromosomes coordinates their capture by microtubules in oocyte meiosis. *The Journal of cell biology* **217**:2661-2674 https://doi.org/10.1083/jcb.201802080 | PubMed

48. **Lenart P.,** Bacher C.P., Daigle N., Hand A.R., Eils R., Terasaki M., Ellenberg J (2005) A contractile nuclear actin network drives chromosome congression in oocytes. *Nature* **436**:812-818 https://doi.org/10.1038/nature03810 | PubMed

49. **Harasimov K.,** Uraji J., Monnich E.U., Holubcova Z., Elder K., Blayney M., Schuh M (2023) Actin-driven chromosome clustering facilitates fast and complete chromosome capture in mammalian oocytes. *Nature cell biology* **25**:439-452 https://doi.org/10.1038/s41556-022-01082-9 | PubMed

50. **Mogessie B.,** Schuh M (2017) Actin protects mammalian eggs against chromosome segregation errors. *Science* **357** https://doi.org/10.1126/science.aal1647 | PubMed

51. **Hernandez B.,** Tetlak P., Domingo-Muelas A., Akizawa H., Skory R.M., Ardestani G., Biro M., Liu X., Bissiere S., Sakkas D., *et al.* (2025) Actin organizes chromosomes and microtubules to ensure mitotic fidelity in the preimplantation embryo. *Science* **388**:eads1234 https://doi.org/10.1126/science.ads1234 | PubMed

52. **Ertych N.,** Stolz A., Stenzinger A., Weichert W., Kaulfuss S., Burfeind P., Aigner A., Wordeman L., Bastians H (2014) Increased microtubule assembly rates influence chromosomal instability in colorectal cancer cells. *Nature cell biology* **16**:779-791 https://doi.org/10.1038/ncb2994 | PubMed

53. **Rata S.,** Suarez Peredo Rodriguez M.F., Joseph S., Peter N., Echegaray Iturra F., Yang F., Madzvamuse A., Ruppert J.G., Samejima K., Platani M., *et al.* (2018) Two Interlinked Bistable Switches Govern Mitotic Control in Mammalian Cells. *Current biology : CB* **28**:3824-3832.e3826. https://doi.org/10.1016/j.cub.2018.09.059 | PubMed

54. **Arakawa H.,** Lodygin D., Buerstedde J.M (2001) Mutant loxP vectors for selectable marker recycle and conditional knock-outs. *BMC Biotechnol* **1** https://doi.org/10.1186/1472-6750-1-7 | PubMed

55. **Schneider C.A.,** Rasband W.S., Eliceiri K.W (2012) NIH Image to ImageJ: 25 years of image analysis. *Nature methods* **9**:671-675 https://doi.org/10.1038/nmeth.2089 | PubMed

56. **Cohen-Sharir Y.,** McFarland J.M., Abdusamad M., Marquis C., Bernhard S.V., Kazachkova M., Tang H., Ippolito M.R., Laue K., Zerbib J., *et al.* (2021) Aneuploidy renders cancer cells vulnerable to mitotic checkpoint inhibition. *Nature* **590**:486-491 https://doi.org/10.1038/s41586-020-03114-6 | PubMed

Peer reviews

Reviewer #1 (Public review):

Sheidaei and colleagues report a novel and potentially important role for an early mitotic actomyosin-based mechanism, PANEM contraction, in promoting timely congression of chromosomes located at the nuclear periphery, particularly those in polar positions. The manuscript will interest researchers studying cell division, cytoskeletal dynamics, and motor proteins. Although some data overlap with the group's prior work, the authors extend those findings by optimizing key perturbations and performing more detailed analyses of chromosome movements, which together provide a clearer mechanistic explanation. The study also builds naturally on recent ideas from other groups about how chromosome positioning influences both early and later mitotic movements.

Comments on revised version:

In the revised manuscript, organizational issues have been largely resolved. In addition, the inclusion of new experiments in additional cell lines, along with an expanded discussion that places actomyosin contractility in the broader conceptual context of other mechanisms governing chromosome movement, has significantly strengthened the manuscript.

https://doi.org/10.7554/eLife.110952.2.sa2

Reviewer #3 (Public review):

Sheidaei et al. report how chromosomes are favourably positioned to facilitate kinetochore-microtubule interactions during early mitosis. Studying kinetochore capture during early prophase is extremely difficult due to kinetochore crowding, but the team has taken up the challenge by classifying types of kinetochore movements, carefully marking kinetochore positions in early mitosis, and linking these to map their fate/next positions over time. The work is an excellent addition to the chromosome segregation field, as most of the literature has thus far focused on tracking kinetochores at slightly later stages of mitosis. The authors show that PANEM facilitates chromosome positioning toward the interior of the newly forming spindle, which in turn promotes chromosome congression. In the absence of PANEM,

chromosomes end up in unfavourable locations and fail to form proper kinetochore-microtubule interactions. The work highlights the perinuclear actomyosin network in early mitosis (PANEM) as a key spatial and temporal element of chromosome congression, a step that precedes the segregation process.

Comments on revised version:

The authors' revisions have brought clarity to the description of movements in many of the figures. The manuscript ties a fundamental process to differences in cancer cell lines.

The work extends their published discovery that an actomyosin network forms on the cytoplasmic side of the nuclear envelope during prophase. The current manuscript explains how this network facilitates chromosome capture and congression by tracking the motions of individual kinetochores during early mitosis. The findings are broadly useful for the cell division and cytoskeletal fields.

https://doi.org/10.7554/eLife.110952.2.sa1

Author response:

The following is the authors' response to the original reviews

> ***Reviewer #1 (Evidence, reproducibility and clarity):***
>
> *Summary*
>
> *Sheidaei and colleagues report a novel and potentially important role for an early mitotic actomyosinbased mechanism, PANEM contraction, in promoting timely congression of chromosomes located at the nuclear periphery, particularly those in polar positions. The manuscript will interest researchers studying cell division, cytoskeletal dynamics, and motor proteins. Although some data overlap with the group's prior work, the authors extend those findings by optimizing key perturbations and performing more detailed analyses of chromosome movements, which together provide a clearer mechanistic explanation. The study also builds naturally on recent ideas from other groups about how chromosome positioning influences both early and later mitotic movements.*
>
> *In its current form, however, the manuscript is not acceptable for publication. It suffers from major organizational problems, an overcrowded and confusing Results section and figures, and a lack of essential experimental controls and contextual discussion. These deficiencies make it difficult to evaluate the data and the authors' conclusions. A substantial structural revision is required to improve clarity and persuasiveness. In addition, several key control experiments and more conceptual context are needed to establish the specificity and relevance of PANEM relative to other microtubule- and actin-based mitotic mechanisms. Testing PANEM in additional cell lines or contexts would also strengthen the claim. I therefore recommend Major Revision, addressing the structural, conceptual, and experimental issues detailed below.*
>
> *Major Comments*
>
> *A. Structural overhaul and figure reorganization*
>
> *The Results section is overly dense, lacks clear structure, and includes descriptive content that belongs in the Methods. Many figure panels should be moved to Supplementary Materials. A substantial reorganization is required to transform the manuscript into a focused, "Reports"-type article.*

> *Move methodological and descriptive details (e.g., especially from the second Results subheading and Figure 2) to the Methods or Supplementary Materials.*

In these parts, we define four phases of kinetochore motion in early mitosis. Without such a description in the main text, readers would be confused about subsequent analyses. Figure 2 is also important to show examples of how the four phases develop. Although we respect this suggestion from the reviewer, we would like to keep these parts in the main text and main figure.

> *Remove repetitive statements that simply restate that later phenotypes arise as consequences of delayed Phase 1 (applicable to subheadings 3 onward).*

As suggested, we have removed the statement for the delayed start of Phase 2 for peripheral kinetochores in azBB-treated cells (Page 9, second paragraph). We have also simplified the statement for the delayed start of Phase 3 and Phase 4 to avoid repetition (Page 9, third paragraph; Page 10, second paragraph).

> *Figure 4I: This panel is currently unclear and should be drastically simplified.*

Following this suggestion, we simplified Figure 4I by removing the column of 'Start', which is easily deduced from the 'Duration' results and therefore does not provide much new information.

> *I recommend to reorganize figures as follows:*
>
> *Figure I: Keep as single figure but simplify. Figure 1D and 1E could be combined, move unnormalized SCV to supplementary materials. Same goes for 1F.*

We have reorganized Figure 1, as suggested, and moved unnormalized data to supplemental materials.

> *New Figure 2: Combine current Figures 2A, 3A, 3C, 3D, 4C, 4F, and 4H to illustrate how PANEM contraction facilitates initial interactions of peripheral chromosomes with spindle microtubules which increases speed of congression initiation.*

If we were to follow this suggestion, we would lose Figure 2B, D, Figure 3B and Figure 4A, where examples of kinetochore motions are shown in images and 3D diagrams. The new Figure would mostly consist of only graphs. Without examples of images and 3D diagrams, readers would have difficulty understanding the study. Although we respect this suggestion from the reviewer, we would like to keep Figures 2, 3 and 4, as they are (except for making Figure 4I simpler; see above).

> *New Figure 3: Combine current Figures 5A, 5C, 5D, 5F, 6B, 6C, and lower panels of 4H to show how*

PANEM contraction repositions polar chromosomes and reduces chromosome volume in early mitosis to enable rapid initiation of congression.

If we were to follow this suggestion, we would lose Figure 5B and Figure 6A, where examples of kinetochore/chromosome dynamics are shown in images and 3D diagrams. For the same reason as above, we would like to keep Figure 5 and 6 as they are, although we respect this suggestion from the reviewer.

> *New Figure 4: Combine Figures 7A, 7B, 7D, 7E, 7F, expanded Supplementary Figure S7, and new data to demonstrate that PANEM actively pushes peripheral chromosomes inward which is important for efficient chromosome congression in diverse cellular contexts.*

We have conducted new experiments to demonstrate the role of PANEM in diverse cellular contexts, as detailed below. We have combined the new results with the original Figure S7 to create Figure 8 in line with this suggestion.

On the other hand, in our view, combining Figure 7A-E and the extended Figure S7 would be confusing because the two parts address different topics. Although we respect this suggestion from the reviewer, we would like to keep Figure 7 and the extended Figure S7 (i.e. Figure 8) separate.

> *B. Specificity and redundancy of actin perturbation*
>
> *To establish the specificity and relevance of PANEM, the authors should include or discuss appropriate controls:*
>
> *Apply global actin inhibitors (e.g., cytochalasin D, latrunculin A) to disrupt the entire actin cytoskeleton. These perturbations strongly affect mitotic rounding and cytokinesis but only modestly influence early chromosome movements, as reported previously (Lancaster et al., 2013; Dewey et al., 2017; Koprivec et al., 2025). The minimal effect of global inhibition must be addressed when proposing a localized actomyosin mechanism. Comment if the apparent differences in this approach and one that the authors were using arises due to different cell types.*

We did experiments along this line, using a dominant-negative LINC construct, in our previous study (Booth et al eLife 2019). LINC-DN should more specifically remove/reduce PANEM than the global actin inhibitors mentioned above. LINC-DN attenuated the reduction of CSV soon after NEBD and increased the number of polar chromosomes (Booth et al eLife 2019); i.e. in this regard, the outcome was similar to azBB treatment in the current study. One can expect that global actin inhibitors would also inhibit the PANEM formation and show effects similar to LINC-DN. By contrast, the indicated references reported that global actin inhibitors strongly affect mitotic rounding and cytokinesis but only modestly influence early chromosome movements, as the reviewer noted. One possibility is that such differences may have arisen from different cell types – this could be important, especially given that some cells form the PANEM and others do not (Figure 8A). A second possibility is that cytokinesis, mitotic rounding and PANEM formation may rely on actin polymerization to different extents. For example, the same concentration of global actin polymerization inhibitors may affect cytokinesis, but may still allow PANEM formation to proceed without observable effects on early chromosome movements. As suggested, we discussed this topic in the Discussion (page 16, third paragraph).

> *Clarify why spindle-associated actin, especially near centrosomes, as reported in prior studies using human cultured cells (Kita et al., 2019; Plessner et al., 2019; Aquino-Perez et al., 2024), was not observed in this study. The Myosin-10 and actin were also observed close to centrosomes during mitosis in X.laevis mitotic spindles (Woolner et al., 2008). Possible explanations include differences in fixation, probe selection, imaging methods, or cell type. Note that some actin probes (e.g., phalloidin) poorly penetrate internal actin, and certain antibodies require harsh extraction protocols. Comment on possibility that interference with a pool of Myo10 at the centrosomes is important for effects on congression.*

As the reviewer implies, we cannot rule out that we could not detect actin associated with the spindle or centrosomes because of the difference in methods or cell lines between the current study and the literature mentioned by the reviewer. We have therefore moderated our claim in the Discussion that 'we did not detect any actin network inside the nucleus, on the spindle or between chromosomes' by adding 'at least, using the method and the cell line in the current study' to this statement (Page 14, second paragraph). We have also cited the three

references mentioned by the reviewer in the Discussion (Page 14, second paragraph). Regarding Myosin10, azBB (blebbistatin variant) should have negligible effects on class-X myosin, including Myosin-10 (Limouze et al 2004 [PMID 15548862]). It is therefore unlikely that the effects of azBB that we observed in the current study are due to the inhibition of Myosin-10. We have cited Woolner et al 2008 and another paper and discussed this topic in the Discussion (Page 14, second paragraph).

> *C. Expansion of PANEM functional analysis*
>
> *To strengthen the conclusions and broaden the study beyond the group's previous work, PANEM function should be tested in additional contexts (some may be considered optional but important for broader impact): [underlined by authors]*
>
> *Test PANEM function in at least one additional cell line that displays PANEM to rule out cell-line-specific effects.*

As suggested, we have studied the effect of PANEM contraction in cell lines other than U2OS. We have found that when PANEM contraction was inhibited, the reduction in chromosome scattering was diminished in RPE1 cells (new Figure 8B, C). Moreover, we have found that inhibition of PANEM contraction increased polar chromosomes during prometaphase/metaphase in RPE1 and HCT116 cells (which form PANEM), but not in HeLa cells (which do not form PANEM) (new Figure 8D, E). These results suggest that the effects of PANEM contraction, originally observed in U2OS cells, are also present in other cell lines (RPE1 and HCT116) that form PANEM.

> *Examine higher-ploidy or binucleated cells to determine whether multiple PANEM contractions are coordinated and if PANEM contraction contributes more in cells of higher ploidies or specific nuclear morphologies.*

This is an interesting suggestion, but it takes lots of time to conduct such a study, and it goes beyond the scope of this paper.

> *Investigate dependency on nuclear shape or lamina stiffness; test whether PANEM force transmission requires a rigid nuclear remnant.*

This is an interesting suggestion, but it takes lots of time to conduct such a study, and it goes beyond the scope of this paper.

> *Analyze PANEM's contribution under mild microtubule perturbations that are known to induce congression problems (e.g., low-dose nocodazole).*

In the current study, we found that PANEM contraction affects chromosome motions in Phase 1 and Phase 3 but not Phase 2 or Phase 4. Mild microtubule perturbation itself could affect chromosome motions in all four Phases. We do not think it would be so informative to study what additional effects the reduced PANEM contraction shows when combined with mild microtubule perturbation.

> *Evaluate PANEM contraction role in unsynchronized U2OS cells, where centrosome separation can occur before NEBD in a subset of cells (Koprivec et al., 2025), and in other cell types with variable spindle elongation timing.*

Following this suggestion, we first investigated the timing of spindle elongation, relative to NEBD, in asynchronous U2OS cells (Figure 8 – figure supplement 3). We imaged cells every 5 min (it was difficult to reasonably observe enough mitotic cells using a shorter interval). Most of the cells showed no significant change in the spindle length (distance between two spindle poles) after (or around) NEBD [e.g. Cell 1 in A] or a mild reduction in it [e.g. Cell 2 in A]. Only a small number of cells (2-3 out of 26) showed a mild increase in the spindle length after (or around) NEBD [e.g. Cell 3 in A]. Because the spindle elongation after NEBD was rare and mild,

it was difficult to address how the timing of spindle elongation affects the effect of PANEM on reducing chromosome scattering and on chromosome relocation from polar regions. We explained this result and discussed this topic in the Discussion section.

> *Quantify not only the percentage of affected cells after azBB but also the number of chromosomes per cell with congression defects in the current and future experiments.*

It is tricky to count the number of chromosomes because they frequently overlap. Counting kinetochores is more feasible, but kinetochore signals show some non-specific background (e.g. those outside of the nucleus in prophase). We therefore quantified the chromosome volume at polar regions in azBB-treated cells (Figure 6C).

> *D. Conceptual integration in Introduction and Discussion*
>
> *The manuscript should better situate its findings within the context of early mitotic chromosome movements:*
>
> *Clearly state in the Introduction and elaborate in the Discussion that initiation of congression is coupled to biorientation (Vukušić & Tolić, 2025). This provides essential context for how PANEM-mediated nuclear volume reduction supports efficient congression of polar chromosomes.*

It has been a widely accepted view in the field that chromosome congression precedes biorientation, since the publication in 2006 (Kapoor et al Science 2006). Very recently, this view has been challenged by the new publication (Vukušić & Tolić, Nat comm 2025), as indicated by this reviewer. We have mentioned this new model and discussed the new interpretation of our results based on this new model, in the Discussion (page 15; 'It has been a widely accepted view…').

To explain the new interpretation of our results more clearly, we have a new diagram as a supplemental figure (Figure 9 – figure supplement 1) in the revised manuscript.

> *Explain that PANEM is most critical for polar chromosomes because their peripheral positions are unfavorable for rapid biorientation (Barišić et al., 2014; Vukušić & Tolić, 2025).*

We have included such a statement in the Discussion, as a part of the new interpretation of our results based on the new model that chromosome biorientation precedes congression (see above). We have also cited the indicated two papers.

> *Discuss how cell lines lacking PANEM (e.g., HeLa and others) nonetheless achieve efficient congression, and what alternative mechanisms compensate in the absence of PANEM. For example, it is well established that cells congress chromosomes after monastrol or nocodazole washout, which essentially bypasses the contribution of PANEM contraction.*

Following this suggestion, we discussed three possible mechanisms that could compensate for a lack of PANEM and facilitate kinetochore-MT interaction and chromosome congression, based on previous literature (Page 17): 1) the enhanced assembly rate of spindle MTs may facilitate kinetochore-MT interactions in N-CIN+ cancer cells, 2) chromosome biorientation may precede congression more frequently to promote the congression towards the spindle midplane, and 3) the balance between CENP-E, Dynein and chromokinesin's activities may incline to greater chromosome-arm ejection forces towards the spindle midplane.

> *Minor Comments*
>
> *These issues are more easily addressable but will significantly improve clarity and presentation.*

> *Introduction*
>
> *Remove the reference to Figure 1A in the Introduction. The portion of Figure 1 and related text that recapitulates the authors' previous work should be incorporated into the Introduction, not the Results.*

As suggested in the second sentence of this comment, we have moved most of the second paragraph of the first section of Results to Introduction (Page 4) and cited Figure 1A and 1B in Introduction. We would like to keep the reference to Figure 1A in the Introduction, because showing the PANEM images at the beginning of the manuscript would help readers' understanding of our study. In addition, citing Figure 1A in the Introduction is more consistent with the suggestion in the second sentence of this comment.

> *Results (by subheading)*
>
> *First subheading: When introducing the ~8-minute early mitotic interval, cite additional studies that have characterized this period: Magidson et al., 2011 (Cell); Renda et al., 2022 (Cell Reports); Koprivec et al., 2025 (bioRxiv); Vukušić & Tolić, 2025 (Nat Commun); Barišić et al., 2013 (Nat Cell Biol).*

As suggested, we cited these references at the indicated part of the first section of the Results (page 5).

> *Second subheading: Cite key reviews and foundational research on kinetochore architecture and sequential chromosome movement during early mitosis: Mussachio & Desai, 2017 (Biology); Itoh et al., 2018 (Sci Rep); Magidson et al., 2011 (Cell); Vukušić & Tolić, 2025 (Nat Commun); Koprivec et al., 2025 (bioRxiv); Rieder & Alexander, 1990 (J Cell Biol); Skibbens et al., 1993 (J Cell Biol); Kapoor et al., 2006 (Science); Armond et al., 2015 (PLoS Comput Biol); Jaqaman et al., 2010 (J Cell Biol).*

Rieder & Alexander, 1990 (J Cell Biol) and Kapoor et al., 2006 (Science) have already been cited in the second section of the Results in the original manuscript. We agree that all other references should be cited in this manuscript, and they are now cited in the Introduction and/or Discussion where they fit best (e.g. Mussachio & Desai 2017 reviews the kinetochore in general and is therefore best cited in the Introduction).

> *Third subheading: Clarify why some kinetochores on Figure 3A appear outside the white boundaries if these boundaries are intended to represent the nuclear envelope.*

We interpret that these are background signals in the cytoplasm, which do not come from kinetochores, because 1) before NEBD, they were outside of the nucleus, and 2) after NEBD, they did not show any characteristic kinetochore motions such as those towards a spindle pole (Phase 2) and the spindle mid-plane (Phase 4). We have commented on these background signals in the legend for Figure 3A.

> *Fourth subheading: Note that congression speed is lower for centrally located kinetochores because they achieve biorientation more rapidly (Barišić et al., 2013, Nat Cell Biol; Vukušić & Tolić, 2025, Nat Commun).*

Relevant to this comment, there was an error regarding the congression speed of central kinetochores (original Figure 4H). The congression speed of peripheral kinetochores was shown correctly, but for central kinetochores it was shown incorrectly with μm per time interval (30s) shown, rather than μm per minute. We amended this error in the revised manuscript (new Figure 4H). Based on the corrected data, the speed of congression is similar between peripheral and central kinetochores. The original Figure 3G (the speed of poleward motion for central kinetochores) had a similar error, which we have also corrected in the revised manuscript. We apologize for these errors and the confusion it may have caused.

Regarding this comment, if biorientation is achieved more rapidly for central kinetochores, Phase 3 (rather than congression speed) would be shorter for central kinetochores. Indeed, Phase 3 is slightly shorter for central kinetochores (control) than for peripheral kinetochores (control) (Figure 4C), but the difference is not statistically significant (t test; p\=0.21).

> *Fifth subheading: Cite studies on polar chromosome movements: Klaasen et al., 2022 (Nature); Koprivec et al., 2025 (bioRxiv). Clarify that Figure 5F displays only those kinetochores that initiated directed congression movements.*

These two references have already been cited and discussed in this Result section of our original manuscript. However, considering this suggestion, we have discussed more about polar chromosome movements reported by Koprivec et al (page 11). Meanwhile, the reviewer is correct about Figure 5F, and we have clarified this point in the Figure 5F legend.

> *Sixth subheading (currently in Discussion): Move the final paragraph of the Discussion into the Results and expand it with preliminary analyses linking PANEM contraction to congression efficiency across untreated cell types or under mild nocodazole treatment.*

As suggested, we have moved the final paragraph of the Discussion in the original manuscript to make a new final section in the Results in the revised manuscript. Moreover, as suggested, we have studied the outcome of inhibiting PANEM contraction in cell lines other than U2OS (Figure 8 B–E), and have described the new results to the new final section in the Results.

> *Discussion*

1. When discussing cortical actin, cite key reviews on its presence and function during mitosis: Kunda & Baum, 2009 (Trends Cell Biol); Pollard & O'Shaughnessy, 2019 (Annu Rev Biochem); Di Pietro et al., 2016 (EMBO Rep).

As suggested, we have cited all these review papers in the Discussion (page 17), and mentioned the role of the cortical actin on the spindle orientation and positioning (Kunda & Baum, 2009; Di Pietro et al., 2016), as well as the function of the actomyosin ring on cytokinesis (Pollard & O'Shaughnessy, 2019).

> *Significance*
>
> *Advance*
>
> *This study's main strength is its novel and potentially important demonstration that contraction of PANEM, a peripheral actomyosin network that operates contracts early mitosis, contributes to the timely initiation of chromosome congression, especially for polar chromosomes. While PANEM itself was previously described by this group, this manuscript provides new mechanistic evidence, improved perturbations, and detailed chromosome tracking. To my knowledge, no prior studies have mechanistically connected this contraction to polar chromosome congression in this level of detail. The work complements dominant microtubule-centric models of chromosome congression and introduces actomyosin-based forces as a cooperating system during very early mitosis. However, the impact of the study is currently limited by major organizational*

> *issues, insufficient controls, and incomplete contextualization within existing literature. Addressing these issues will substantially improve clarity and credibility. [underlined by authors]*

We have addressed the underlined criticisms as detailed above.

> *Audience*
>
> *Primary audience of this study will be researchers working in cell division, mitosis, cytoskeleton dynamics, and motor proteins. The findings may interest also the wider cell biology community, particularly those studying chromosome segregation fidelity, spindle mechanics, and cytoskeletal crosstalk. If validated and clarified, the concept of PANEM could be integrated into textbooks and models of chromosome congression and could inform studies on mitotic errors and cancer cell mechanics.*
>
> *Expertise*
>
> *My expertise lies in kinetochore-microtubule interactions, spindle mechanics, chromosome congression, and mitotic signaling pathways.*
>
> ***Reviewer #2 (Evidence, reproducibility and clarity):***
>
> *In this manuscript, Sheidaei et al. reported on their study of chromosome congression during the early stages of mitotic spindle assembly. Building on their previous study (ref. #15, Booth et al., Elife, 2019), they focused on the exact role of the actin-myosin-based contraction of the nuclear envelope. First, they addressed a technical issue from their previous study, finding a way to specifically impair the actomyosin contraction of the nuclear membrane without affecting the contraction of the plasma membrane. This allowed them to study the former more specifically. They then tracked individual kinetochores to reveal which were affected by nuclear membrane contraction and at what stage of displacement towards the metaphase plate. The investigation is rigorous, with all the necessary controls performed. The images are of high quality. The analyses are accurate and supported by convincing quantifications. In summary, they found that peripheral chromosomes, which are close to the nuclear membrane, are more influenced by nuclear membrane contraction than internal chromosomes. They discovered that nuclear membrane contraction primarily contributes to the initial displacement of peripheral chromosomes by moving them towards the microtubules. The microtubules then become the sole contributors to their motion towards the pole and subsequently the midplane. This step is particularly critical for the outermost chromosomes, which are located behind the spindle pole and are most likely to be missegregated.*
>
> *Significance*
>
> *While the conclusions are somewhat intuitive and could be considered incremental with regard to previous works, they are solid and improve our understanding of mitotic fidelity. The authors had already reported the overall role of nuclear membrane contraction in reducing chromosome missegregation in their previous study, as mentioned fairly and transparently in the text. However, the reason for this is now described in more detail with solid quantification. Overall, this is good-quality work which does not drastically change our understanding of chromosome congression, but contributes to improving it. Personally, I am surprised by the impact of such a small contraction (of around one micron) on the proper capture of chromosomes and wonder whether the signalling associated with the contraction has a local impact on microtubule dynamics. However, investigating this point is clearly beyond the scope of this study, which can be published as it is. [underlined by authors]*

The suggested topic (underlined) is intriguing. However, we agree with the reviewer that it is beyond the scope of this paper. The reviewer recommends publication of our manuscript as it is.

> ***Reviewer #3:***
>
> *Sheidaei et al., report how chromosomes are brought to positions that facilitate kinetochore-microtubule interactions during mitosis. The study focusses on an important early step of the highly orchestrated chromosome segregation process. Studying kinetochore capture during early prophase is extremely difficult due to kinetochore crowding but the team has taken up the challenge by classifying the types of kinetochore movements, carefully marking kinetochore positions in early mitosis and linking these to map their fate/next-positions over time. The work is an excellent addition to the field as most of the literature has thus far focussed on tracking kinetochore in slightly later stages of mitosis. The authors show that the PANEM facilitates chromosome positioning towards the interior of the newly forming spindle, which in turn facilitates chromosome congression - in the absence of PANEM chromosomes end up in unfavourable locations, and they fail to form proper kinetochore-microtubule interactions. The work highlights the perinuclear actomyosin network in early mitosis (PANEM) as a key spatial and temporal element of chromosome congression which precedes the segregation process.*
>
> *Major points*
>
> *(1) The complexity of tracking has been managed by classifying kinetochore movements into 4 categories, considering motions towards or away from the spindle mid-plane. While this is a very creative solution in most cases, there may be some difficult phases that involve movement in both directions or no dominant direction (eg Phase3-like). It is unclear if all kinetochores go through phase1, 2, 3 and 4 in a sequential or a few deviate from this pattern. A comment on this would be helpful. Also, it may be interesting to compare those that deviate from the sequence, and ask how they recover in the presence and absence of azBB.*

To respond to this comment, we would like to first clarify how we selected kinetochores for our analysis. We selected kinetochores that can be individually tracked. If kinetochore tracking was difficult (before the start of Phase 4 in control and azBB-treated cells or before observing the extended Phase 3 in azBB-treated cells) because of kinetochore crowding, we did not choose such kinetochores. For example, related to the next comment of this Reviewer, we did not include kinetochores close to spindle poles (within 4 μm) at NEBD in our analysis for the following two reasons: First, these kinetochores often did not show clear and rapid movements towards a spindle pole, which we used to define Phase 2. Second, although we referred to kinetochore co-localization with a microtubule signal for the start of Phase 2, this was difficult for kinetochores close to spindle poles because of a high density of microtubules. As requested, we have added this comment to the Method section (page 25).

With the above selection, all selected kinetochores without azBB treatment (control) showed the poleward motion (Phase 2) and congression (Phase 4) in this order, though their extents were varied among kinetochores. All selected kinetochores with azBB treatment also showed the poleward motion (Phase 2), and some of them showed congression (Phase 4) after Phase 2. Then, Phase 1 and Phase 3 were defined as intervals between NEBD and Phase 2 and between Phase 2 and Phase 4, respectively. If no Phase 4 was observed with azBB, we judged that Phase 3 continued till the end of tracking. We have added this comment to the Method section (page 25-26).

> *(2) Would peripheral kinetochore close to poles behave differently compared to peripheral kinetochore close to the midplane (figure S4)? In figure 3D, are they separated? If not, would it look different?*

Since we did not include kinetochores close to spindle poles (at NEBD), for which it was difficult to define Phase 2 (see our response to the above major point 1), in our analysis, the suggested comparison is not feasible.

> *(3) Uncongressed polar chromosomes (eg., CENPE inhibited cells) are known to promote tumbling of the spindle. In figure 5B with polar chromosomes, it will be helpful to indicate how the authors decouple spindle pole movements from individual kinetochore movements.*

In contrast to CENPE-inhibited cells, azBB-treated cells did not show much tumbling of the spindle, though both cells showed uncongressed polar chromosomes. The reason for this difference may be fewer uncongressed polar chromosomes in azBB-treated cells. There were still modest spindle motions in azBB-treated cells. However, because kinetochore motions were assessed relative to a spindle pole (and other reference points on the spindle) in our study (Figure 2A, C), the modest spindle motions were offset in our analyses of kinetochore motions. We have clarified the underlined part in the Method section (page 24).

> *(4) The work has high quality manual tracking of objects in early mitosis- if this would be made available to the field, it can help build AI models for tracking. The authors could consider depositing the tracking data and increasing the impact of their work.*

As suggested, we have included kinetochore tracking data as supplemental data in the revised manuscript (Figure 3 – source data 1–4; Figure 5 – source data 1, 2).

> *Minor points*
>
> *(1) It will be helpful for readers to see how many kinetochores/cell were considered in the tracking studies. Figure legends show kinetochore numbers but not cell numbers.*

As suggested, we have now mentioned the number of cells, where the kinetochore motions were analyzed, in the legends for Figures 3, 4, 5, and supplemental figures.

> *(2) Discussion point: If cells had not separated their centrosomes before NEBD, would PANEM still be effective? Perhaps the cancer cell lines or examples as shown in Figure 6A have some clues here.*

Following this suggestion, we first investigated the timing of spindle elongation, relative to NEBD, in asynchronous U2OS cells (Figure 8 – figure supplement 3). We imaged cells every 5 min (it was difficult to reasonably observe enough mitotic cells using a shorter interval). Most of the cells showed no significant change in the spindle length (distance between two spindle poles) after (or around) NEBD [e.g. Cell 1 in A] or a mild reduction in it [e.g. Cell 2 in A]. Only a small number of cells (2-3 out of 26) showed a mild increase in the spindle length after (or around) NEBD [e.g. Cell 3 in A]. Because the spindle elongation after NEBD was rare and mild, it was difficult to address how the timing of spindle elongation affects the effect of PANEM on reducing chromosome scattering and on chromosome relocation from polar regions. We explained this result and discussed this topic in the Discussion section.

> *(3) Figure 7 cartoon shows misalignment leading to missegregation. It may be useful to consider this in the context of the centrosome directed kinetochore movements via pivoting microtubules. Is this process blocked in azBB-treated cells?*

We understand that the Reviewer refers to the kinetochore pivoting mechanism around a spindle pole, which was recently reported by the Tolic group (Koprivec et al., 2026). Such a

pivoting mechanism would work only when the spindle elongates (i.e. the distance between spindle poles is enlarged) after NEBD. Therefore, to address this Reviewer's question, we tried to assess how PANEM contraction contributes to relocating polar chromosomes when the spindle elongates before or after NEBD in asynchronous U2OS cells (i.e. in the situation where the kinetochore pivoting mechanism is applied or not), as we noted above in response to Point 2. However, spindle elongation after NEBD was rare and mild, and we were unable to address this issue (see our response to Point 2). We discussed this matter in the Discussion section.

> *(4) Are all the N-CIN- lines with PANEM highly sensitive to azBB? In other words, is PANEM essential for normal congression in some of these lines.*

Because blebbistatin could kill cells by inhibiting cytokinesis, the blebbistatin sensitivity of cell growth may not necessarily reflect how essential the PANEM contraction is for chromosome congression.

Instead, we addressed more directly how essential the PANEM contraction is for chromosome congression. We analyzed chromosome congression in RPE1 and HCT116 cells (both are NCIN-) in the presence and absence of pnBB, the inhibitor of PANEM contraction (new Figure 8D, E). With pnBB, these cells showed congression defects, suggesting that the PANEM contraction is essential for chromosome congression in these N-CIN- cells.

> *(5) Are congression times delayed in lines that naturally lack PANEM?*

For example, it takes 10-20 min for HeLa cells (lacking PANEM) to complete chromosome congression after the NEBD (Bancroft et al 2025: *https://doi.org/10.1242/jcs.163659*). This is not significantly different from the time (8-18 min) for chromosome congression we observed in U2OS cells (which form PANEM). We assume that cells lacking PANEM have developed a compensatory mechanism for efficient chromosome congression – we have discussed possible compensatory mechanisms in the last paragraph of the Discussion (page 17).

> *(6) Page 23 "we first identified the end of congression" how does this relate to kinetochore oscillations that move kinetochores away from the metaphase plate?*

The start of kinetochore oscillation was defined as the end of Phase 4 if we could track the kinetochore until that point. In some cases where the kinetochore became close to the midplane (< 2.5 μm), it was not possible to track it further due to kinetochore crowding around the spindle mid-plane – in such cases, the end of Phase 4 was assigned as the end of tracking. These definitions were not necessarily clear in the original manuscript. Moreover, in the original manuscript, it was not clearly stated that the end of Phase 4 was defined in the same way for both non-polar and polar kinetochores. We have now clarified these points in the Method section (page 25).

> *(7) Are spindle pole distances (spindle sizes) different in early and late mitotic cells (4min vs 6min after NEBD) in control vs azBB-treated cells? Please comment on Figure S2E (mean distance) in the context of when phase 4 is completed. Does spindle size return to normal after congression?*

In Figure S2E (Figure 1 – figure supplement 6 in the revised manuscript), we did not observe a significant difference in the spindle-pole distance (the spindle size) between control and azBBtreated cells at any individual time points. The smallest p-value was 0.094 at 6.0 min. As suggested, we have explained this in the legend for this supplementary figure. Completion of Phase 4 is highly variable across different kinetochores within the same cell; thus, a general comment on its completion timing in cells is not feasible.

> *Significance:*

The current work builds upon their previous work, in which the authors demonstrated that an actomyosin network forms on the cytoplasmic side of the nuclear envelope during prophase. This work explains how the network facilitates chromosome capture and congression by tracking motions of individual kinetochores during early mitosis. The findings can be broadly useful for cell division and the cytoskeletal fields.

https://doi.org/10.7554/eLife.110952.2.sa0